GEOExplorer

Laboratory for Nuclear Technologies Applied to the Environment

Università degli Studi di Ferrara

Finanziato dall'Unione europea NextGenerationEU

MUR Ministero dell'Università e della Ricerca

A STANDARDIZED CG-5 PROCESSING WORKFLOW FOR INDUSTRIAL AND ENVIRONMENTAL MICROGRAVITY APPLICATION

Tutor:
Prof. Fabio Mantovani

Ph.D. in Physics – Cycle XXXVIII

PhD candidate:
Dario Petrone

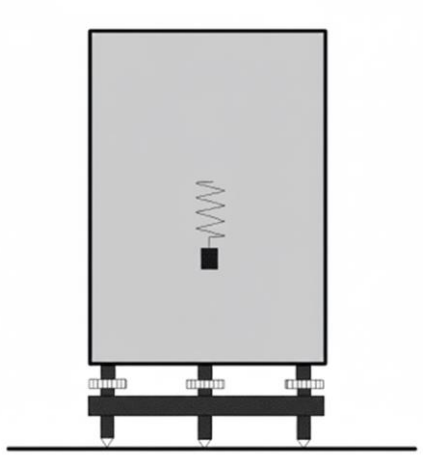

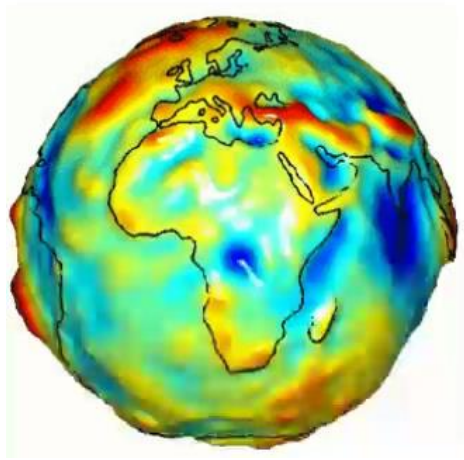

Borsa di Studio finanziata da fondi PNRR ex DM 352 del 09.04.2022 e da GEOexplorer Impresa Sociale Srl

Basis of microgravity

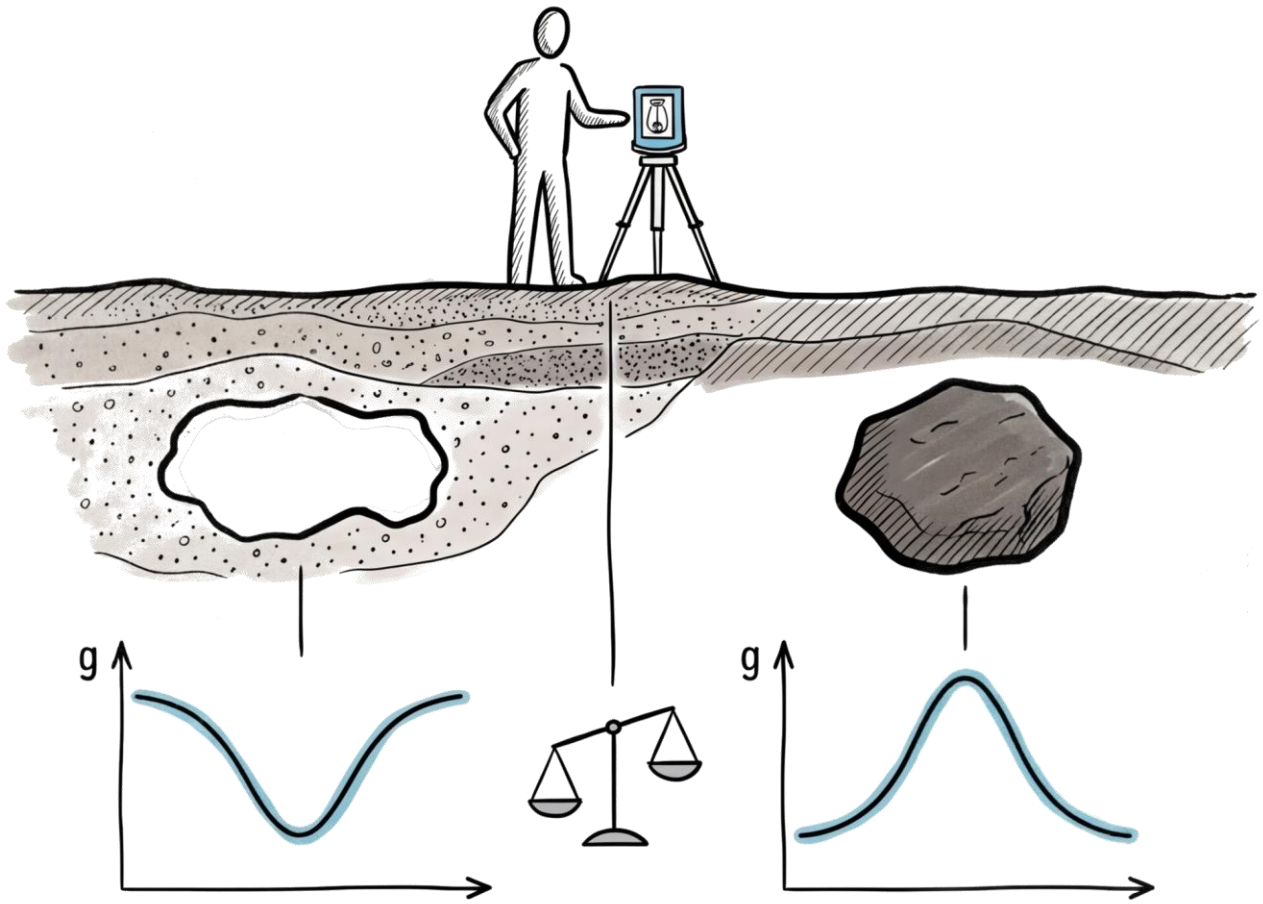

Applied microgravimetry in industrial environments: a PhD pathway

- **Microgravimetric surveying** is a **high resolution geophysical technique** using **relative gravimeters** to measure spatial variations of the Earth gravity field.

- The method quantifies gravity differences at the **µGal level** (1 µGal = 10^{-8} m s^{-2}), allowing detection of **density contrasts** associated with **voids**, **low density zones**, or **high density bodies**.

- Measurements are acquired on **spatial grids** and processed into **residual anomaly maps**, supporting **non invasive detection** of buried structures from near surface to depths of **hundreds of meters**.

Urban environment

Mountainous context

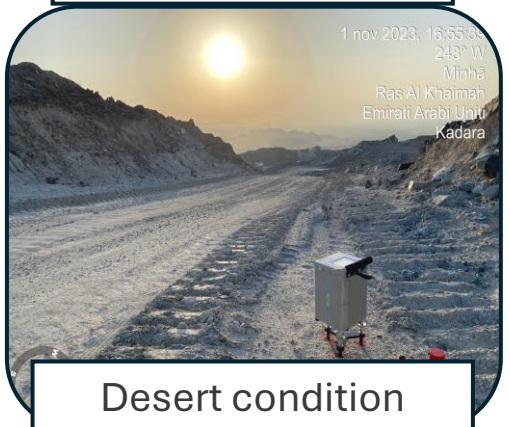

Desert condition

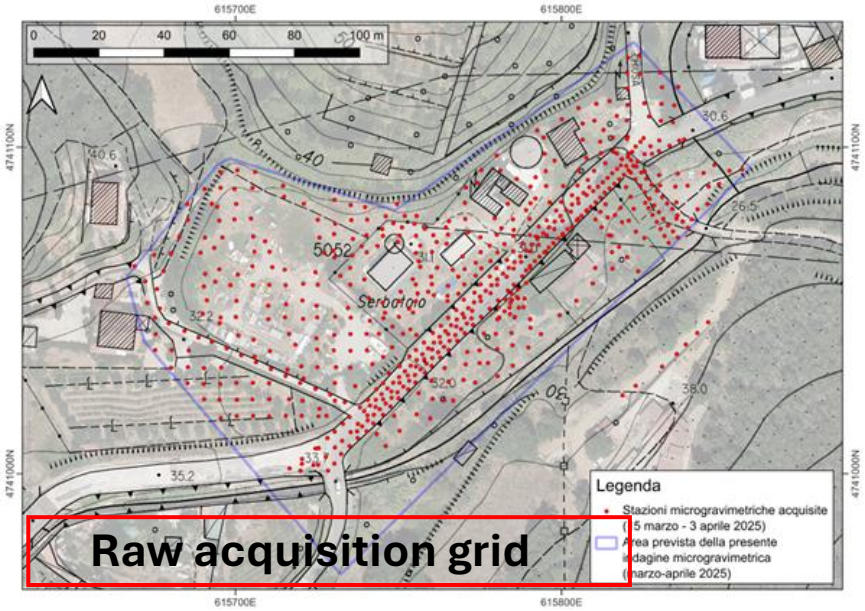

Raw acquisition grid

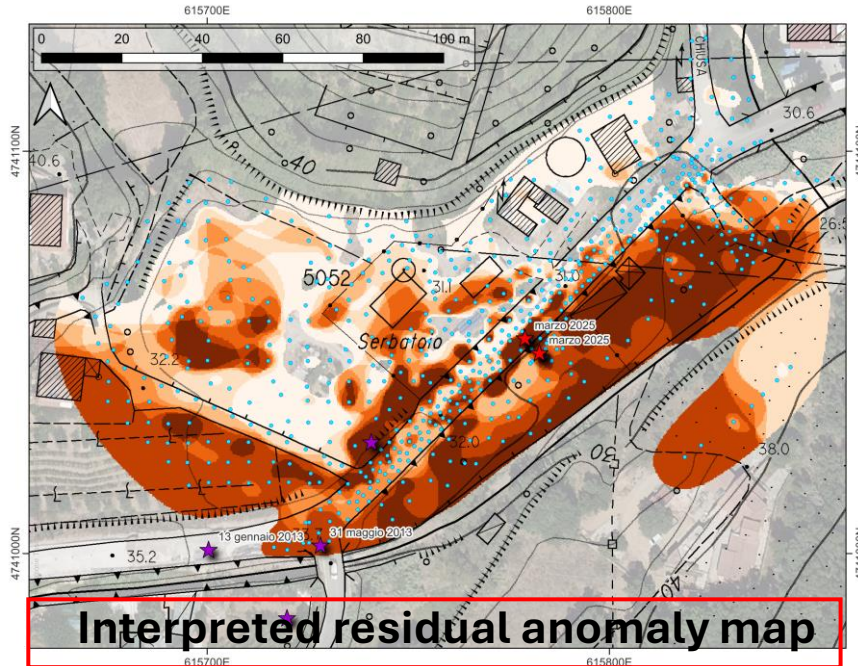

Interpreted residual anomaly map

Technical workflow for microgravity data analysis

The development of a complete workflow to transform noisy field measurements into statistically validated gravity anomalies under real-world operational constraints.

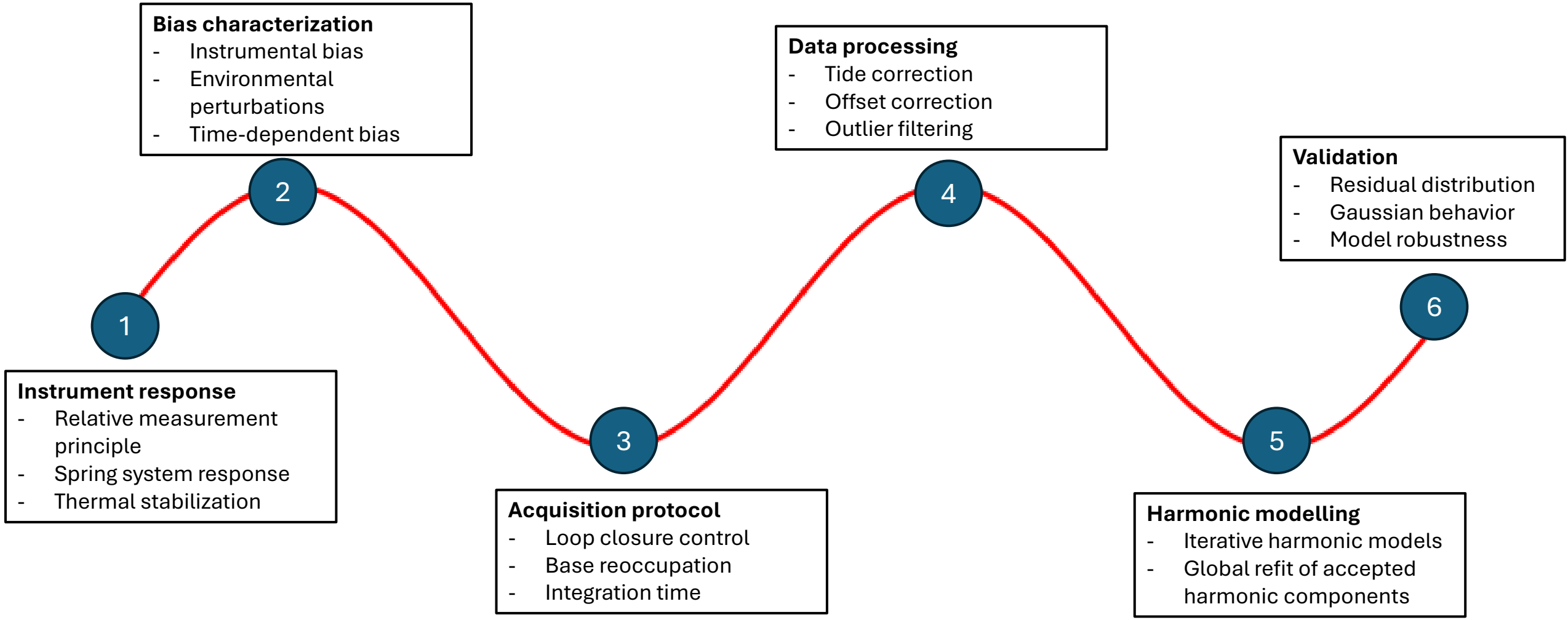

SCINTREX CG5 relative gravimeter: architecture and perfomance

Relative spring gravimeter based on a fused-quartz elastic system.

$\Delta g \propto \Delta x$ (spring elongation)

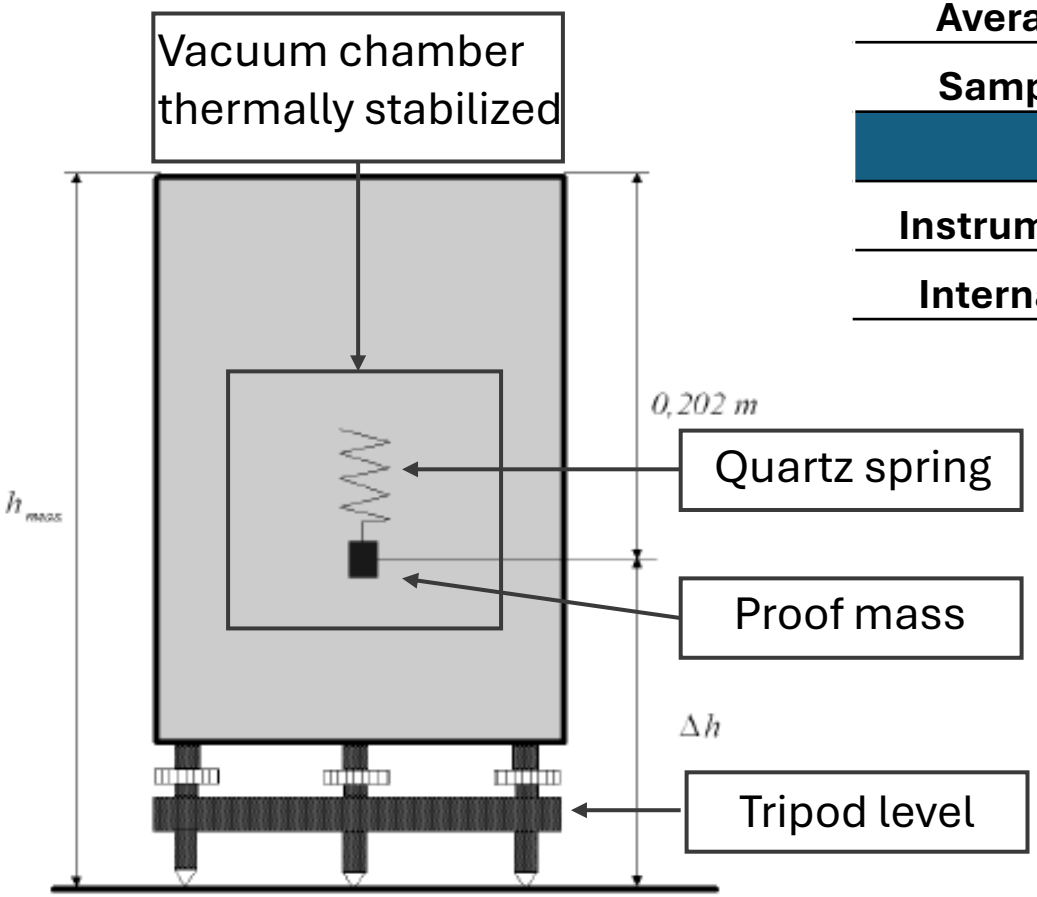

Performance	
Reading Resolution	1 µGal
Repeatability	5 µGal
Acquisition	
Average timing	User-defined (30-120 s)
Sampling Rate	6 Hz digitized samples
Hardware	
Instrument Weight	8.9 kg
Internal Memory	12 MB Flash memory

Instrumental and environmental bias in CG-5 measurements

Microgravity measurements are affected by distinct instrumental and environmental bias components with different physical origins and temporal scales.

Instrumental bias (endogenous)

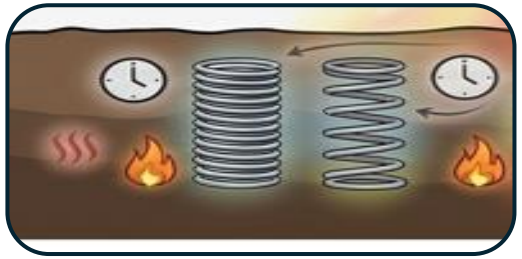

- **Quartz spring creep**
  Spring deformation evolves slowly over time
- **Elastic hysteresis**
  Response depends on previous mechanical states
- **Time-dependent relaxation**
  Signal varies after transport and repositioning
- **Thermal residual effects**
  Temperature influences spring behavior
- **Tilt misalignment**
  Non-vertical axis introduces systematic gravity error

Environmental bias (exogenous)

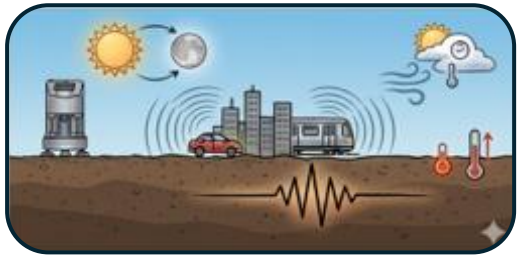

- **Earth tide forcing**
  Sun–Moon system induces periodic gravity variations
- **Microseismic noise**
  Ground vibrations introduce high-frequency measurement fluctuations
- **Anthropogenic vibrations**
  Human activity generates transient noise in signal
- **Thermal gradients**
  Soil–air exchange alters local physical conditions

Field acquisition protocol in microgravity surveys

DESK SURVEY

- Grid spacing by evaluating expected anomalies.
- Field survey preparation.
- Upload grid survey in qfield application.

PRE SURVEY

- 24 h continuous acquisition to estimate long term-drift.
- Transport in the field in a shock-protected case.

BASE STATION

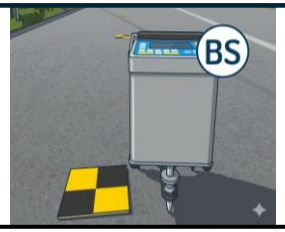

- Stable.
- Noise isolated
- Easily repeatable
- Must be acquired at start and the end of the acquisition minimum.

GRAVITY WORKFLOW

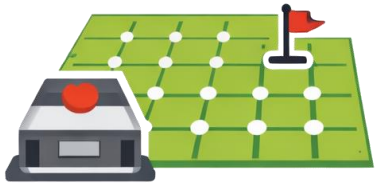

- Loop acquisition
- Integration time (30–120 s)
- Instrument leveling (±10 arcsec)
- If memory CG-5 is full
- Acquire base station
- Download and clearing memory
- Reacquire base station

GNSS WORKFLOW

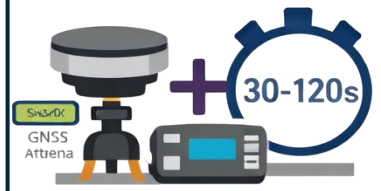

- GNSS RTK positioning
- x – y ~ 10 cm
- z ~ 5 cm

Technological motivations

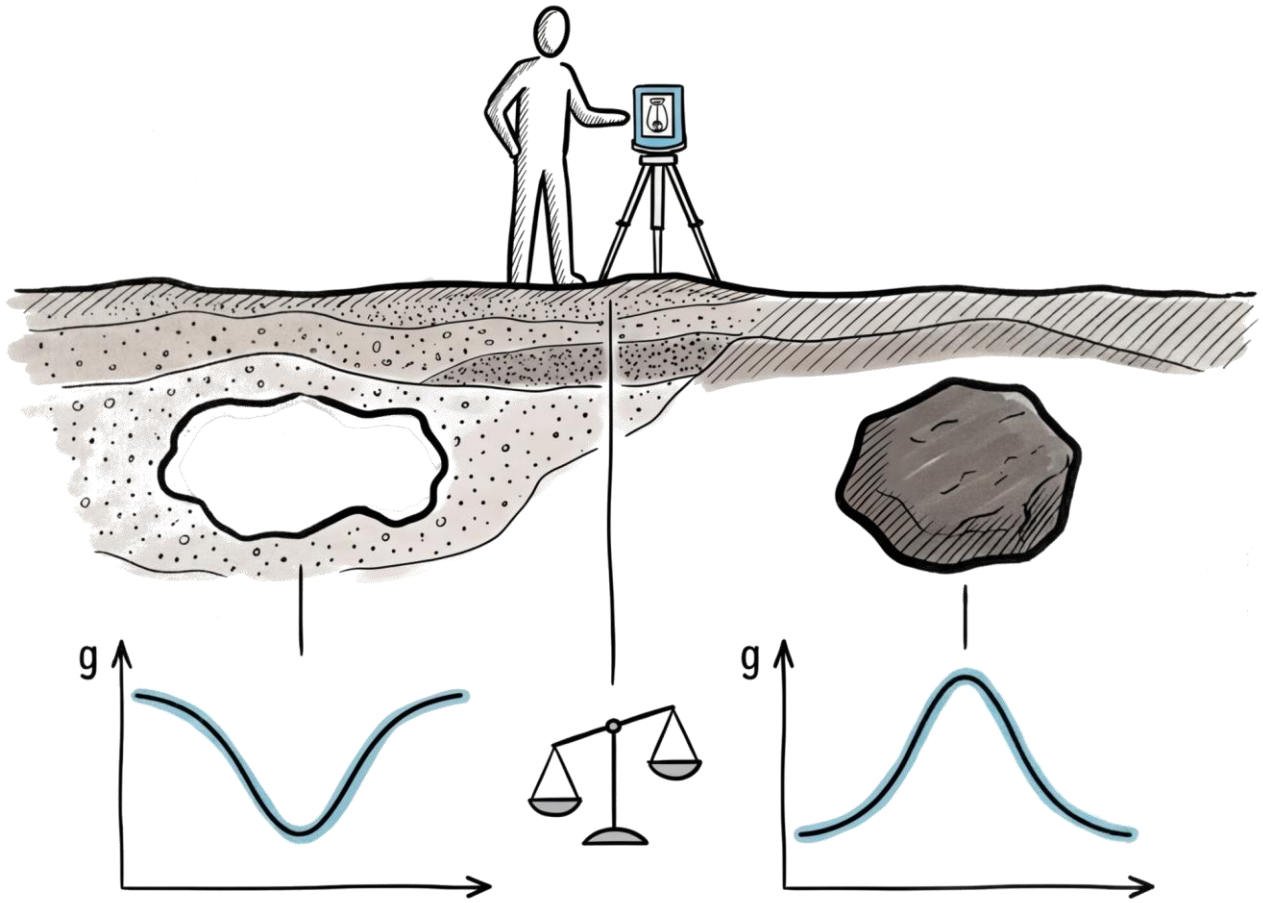

Processing workflow

DATA ACQUISITION

Tide correction

Memory-jump correction

Sistematyc bias correction

TEMPORAL ANALYSIS

Latitude correction

Free air correction

Bouguer correction

SPATIAL ANALYSIS

Sinkhole presences confirmed in low density area

INTERPOLATED MODEL

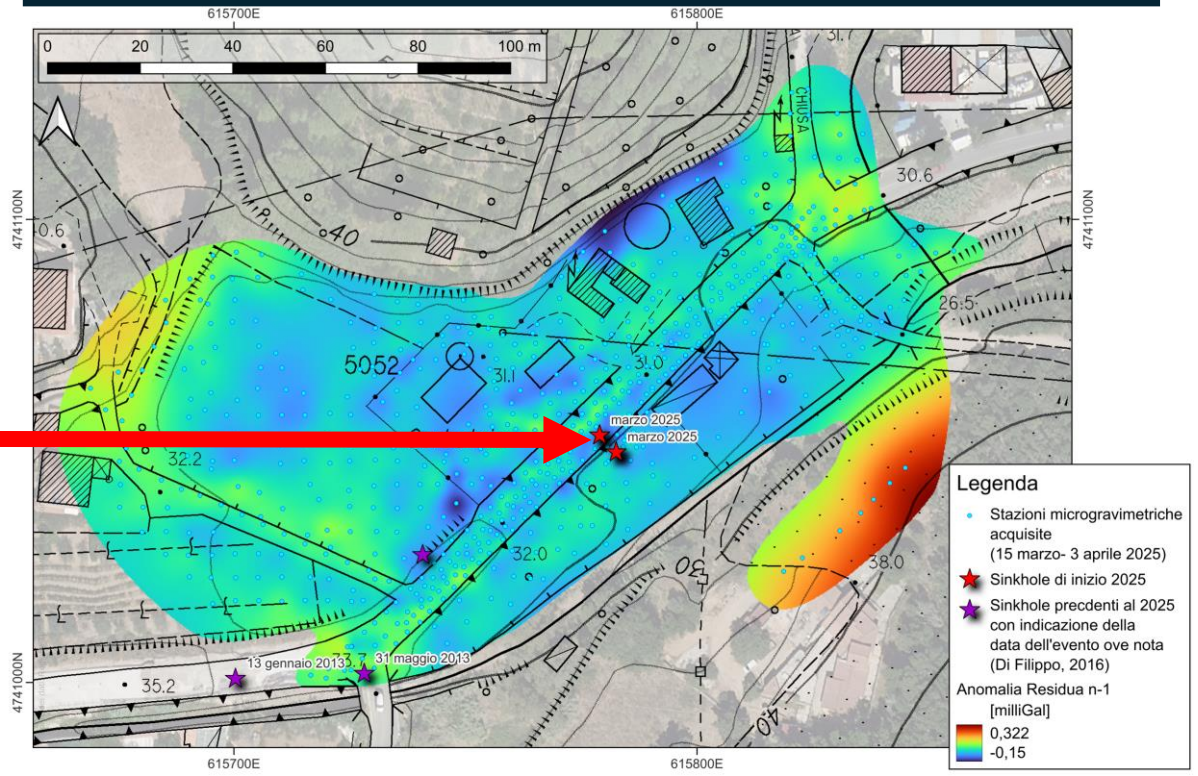

Raw Data After Acquisition: Limited Direct Interpretability

Observed magnitude

- Raw base stations reading before jumps correction show variation around **5000 µGal.**
- Raw base stations reading show variation around **800 µGal**
- Variations up to **200–300 µGal in few hours.**

Impact on detection capability

- Gravity anomalies : **~40–60 µGal.**
- Drift amplitude exceeds signal amplitude

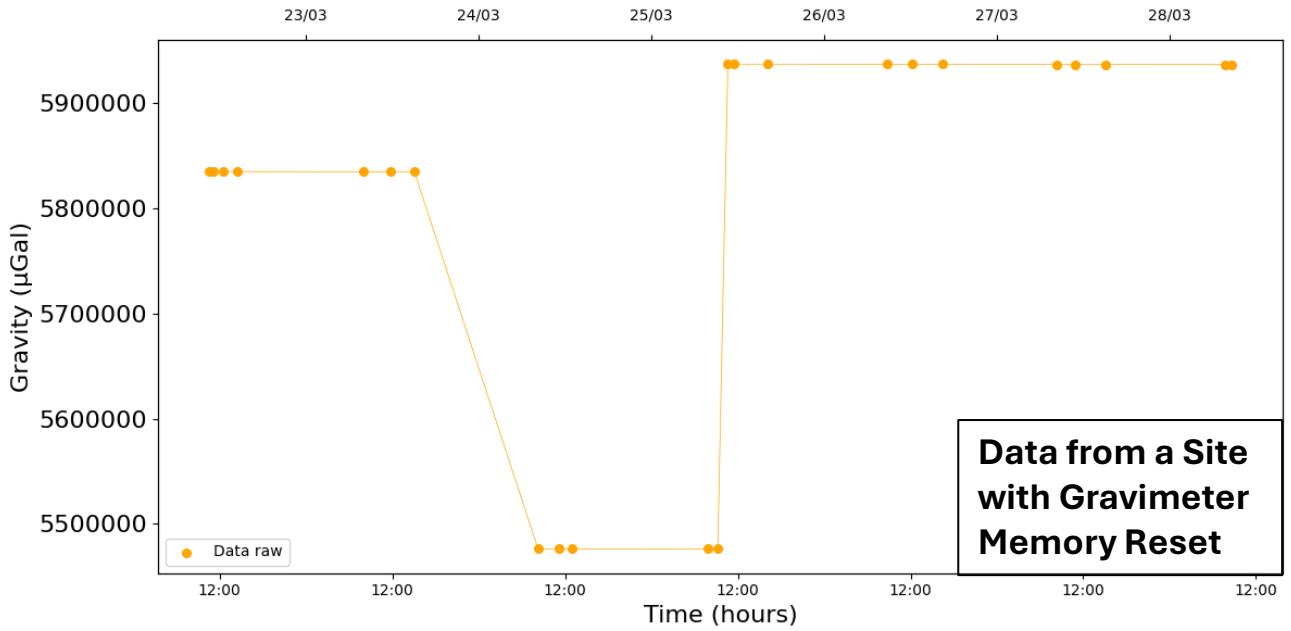

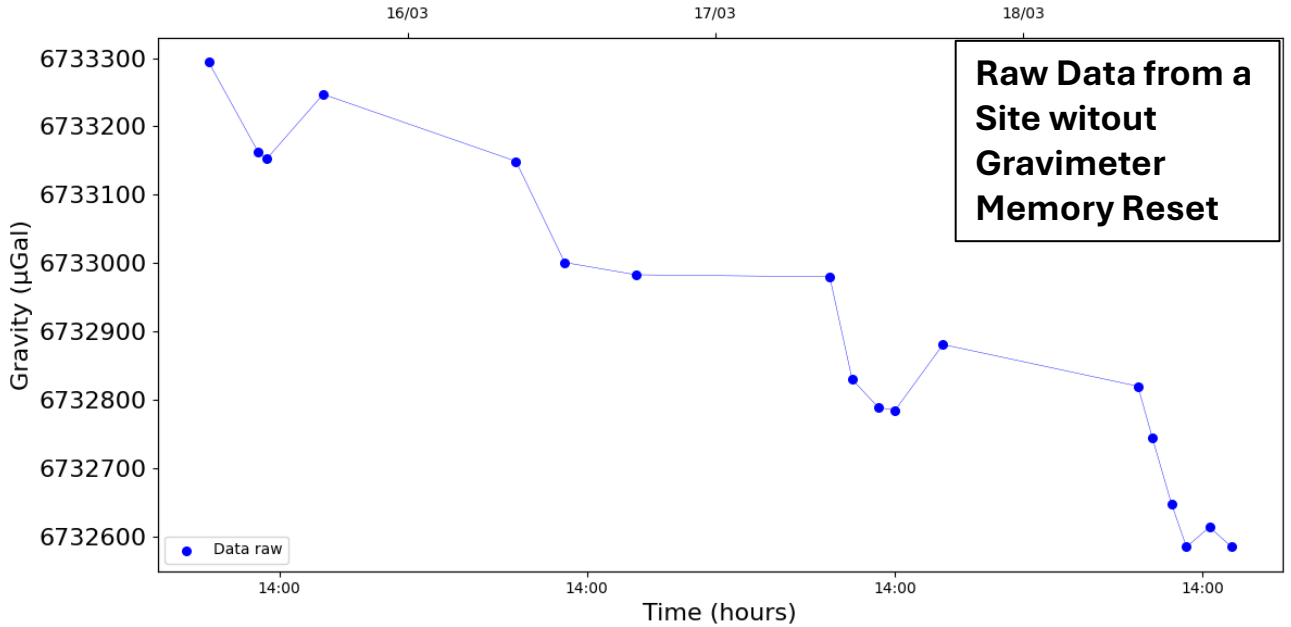

State of the art in instrumental drift correction

Literature shows that instrumental bias is commonly modeled using linear or low-order polynomial functions.

Reference	Acquisition	Drift model	Strengths	Limitations
Seigel, 1995	Base station loops	Linear model	Robust, simple, field-proven	Assumes linear drift, no uncertainty modeling
Debeglia & Dupont, 2002 (standard)	Closed loops	Linear model	Efficient for field surveys	Residual drift and tidal effects remain
Debeglia & Dupont, 2002 (continuous)	Fixed base + mobile	Linear + quadratic	Improved drift representation	Requires dual instruments, complex logistics
Elsaka, 2020	Long-term stationary	High-order polynomial	Captures non-linear drift	Risk of overfitting, not field-adapted
Battaglia et al., 2022	Double-loop network	Weighted least square (WLS)	Uncertainty propagation, improved estimates	Requires dense acquisition, dual instruments

Most existing approaches rely on simplified drift representations that fail to capture the complexity observed in real field conditions.

Analysis pipeline

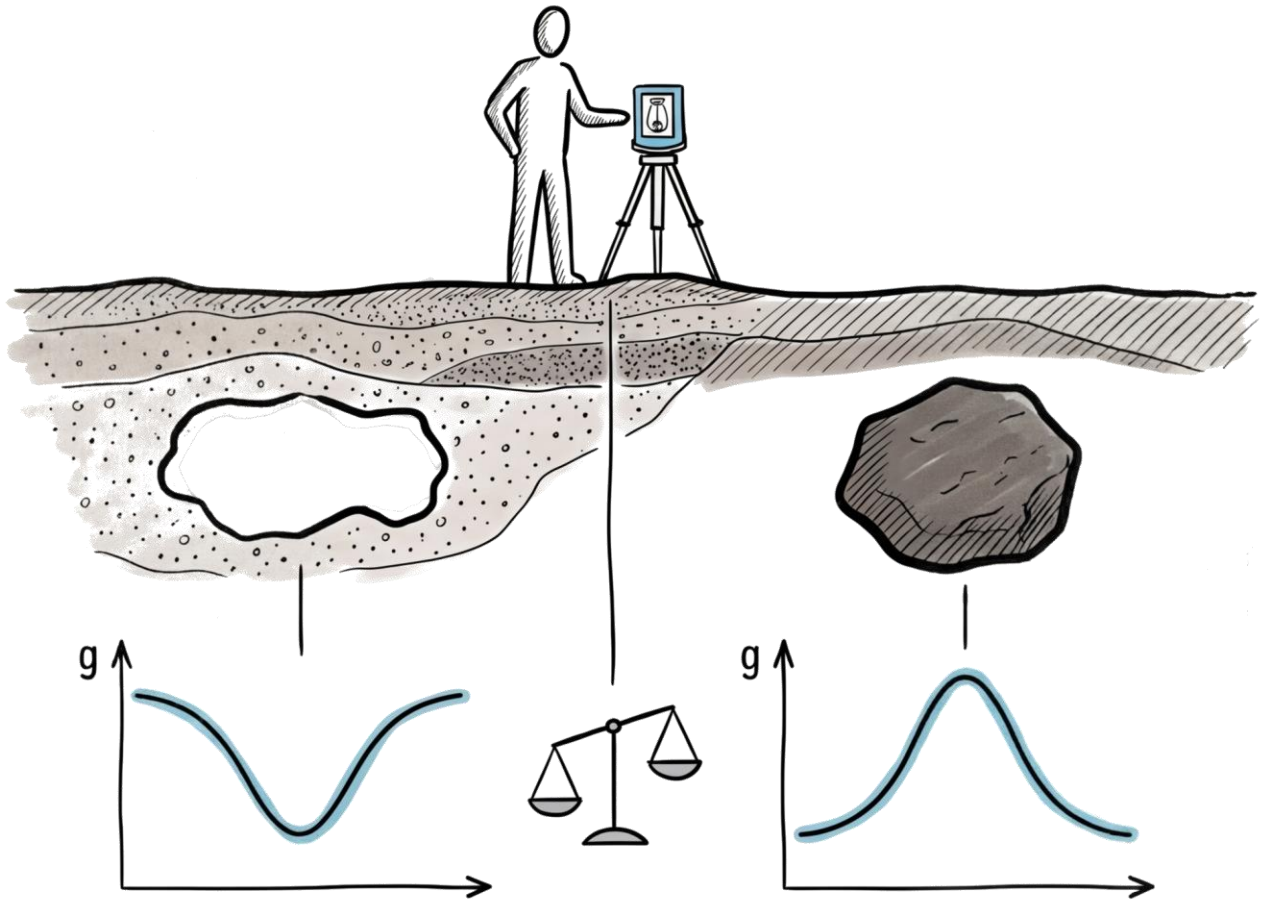

Field datasets and operational scenarios

The workflow was developed and tested on nine datasets spanning a wide range of operational scenarios.

Site ID	Site	Duration [d]	N base station	Site environment	Target
1	Brica di Sillano (Lucca, Italy)	14	29	Mountainous	Cavities detection
2	Pigneto (Rome, Italy)	6	23	Urban	Cavities detection
3	Bagni di Tivoli phase 1 (Rome, Italy)	20	41	Urban	Cavities detection
4	Bagni di Tivoli phase 2 (Rome, Italy)	7	14	Urban	Cavities detection
5	Fujairah (UAE)	43	87	Rocky desert	Mineral exploration
6	Rio Marina (Elba Island, Italy)	12	29	Insular	Sinkhole detection
7	Tivoli (Rome, Italy)	9	37	Urban	Cavities detection
8	Colle Mentuccia (Rome, Italy)	5	14	Urban	Infrastructure modelling
9	Test San Giovanni Valdarno	20	25069	Laboratory	Drift characterizaton

Data processing workflow for bias systematic correction

Given the large dynamic range between raw observations and target anomalies, a dedicated processing workflow is required to isolate the geophysical signal from dominant systematic contributions.

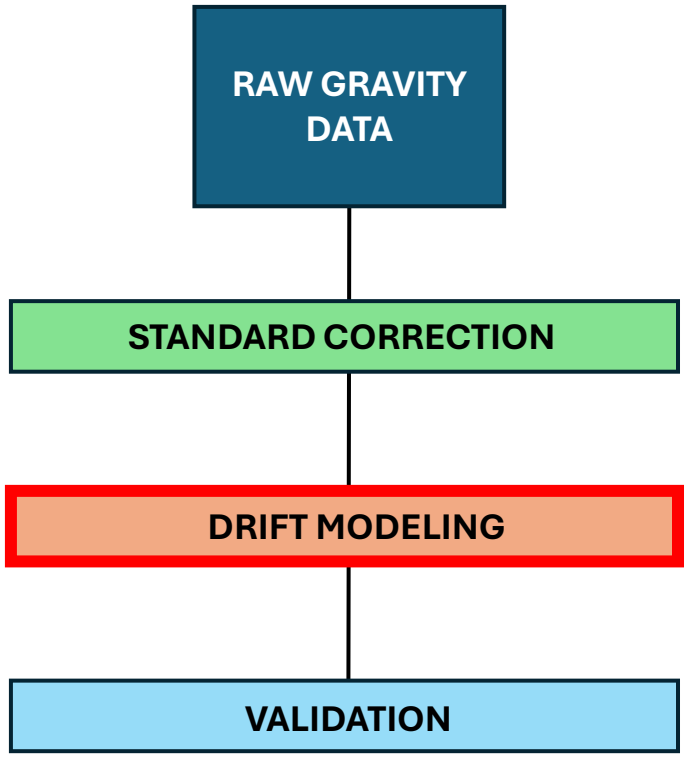

Instrumental noise and measurement variability across surveys

Instrumental noise is quantified across multiple field surveys using the standard deviation of repeated measurements at fixed stations, providing an estimate of the achievable resolution.

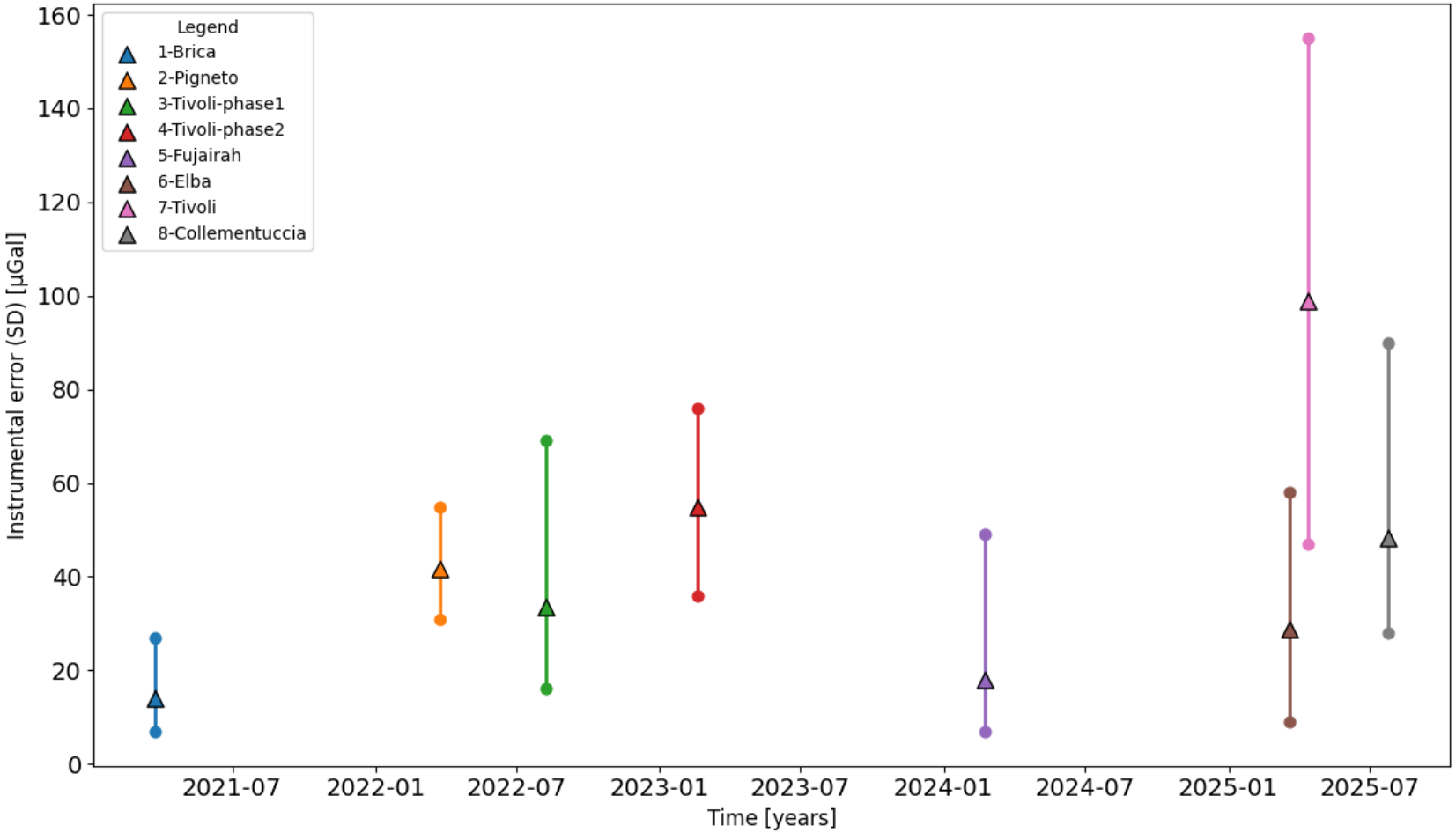

Instrumental noise statistics (SD)

Site ID	Min [µGal]	Max [µGal]	Mean [µGal]
1	7	27	14
2	31	55	42
3	16	69	33
4	36	76	55
5	7	49	18
6	9	58	29
7	47	155	99
8	28	90	48

Tide correction

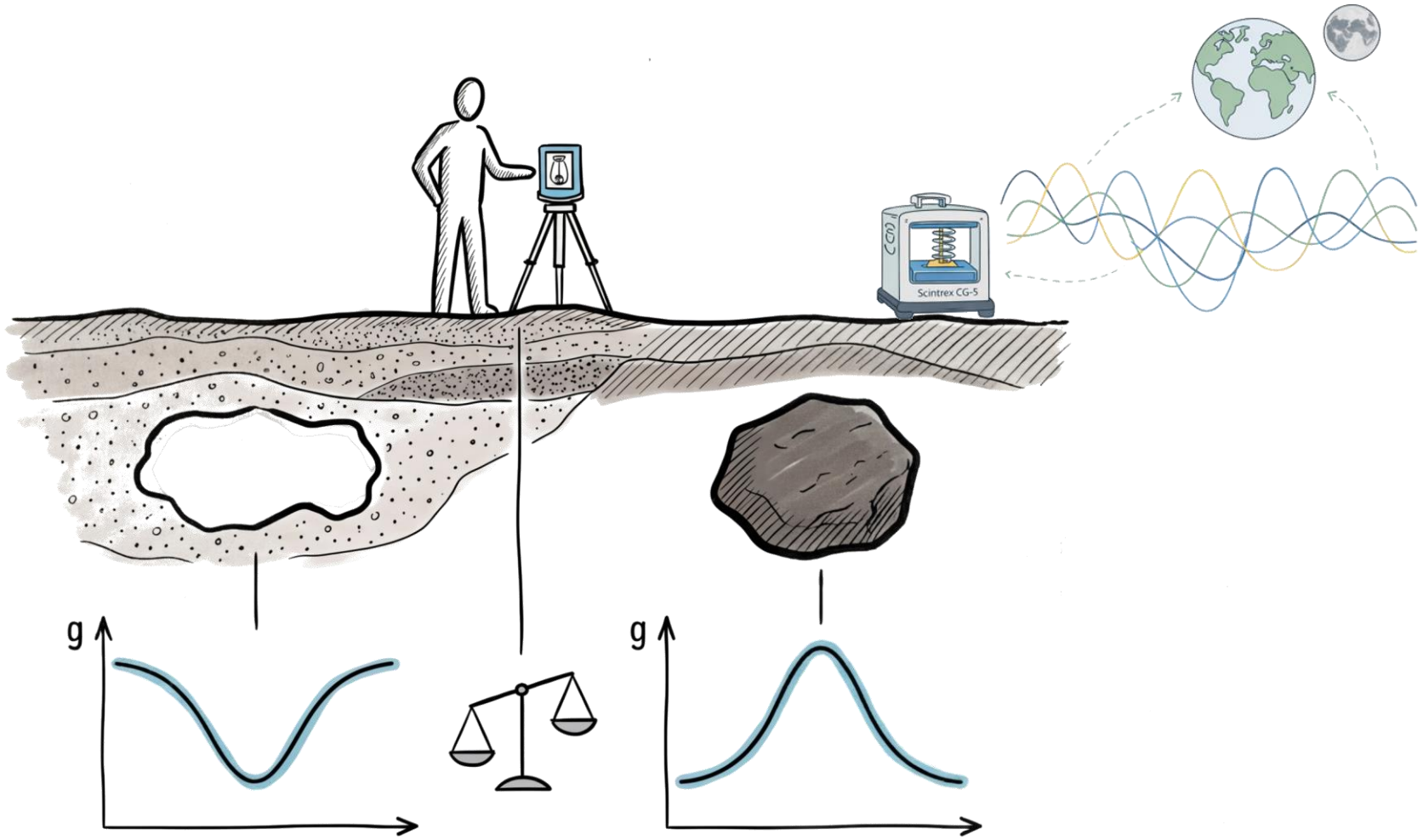

Raw gravity time series: systematic bias and daily variability

Raw gravity time series from the laboratory are dominated by systematic bias and periodic daily fluctuations, masking the target signal.

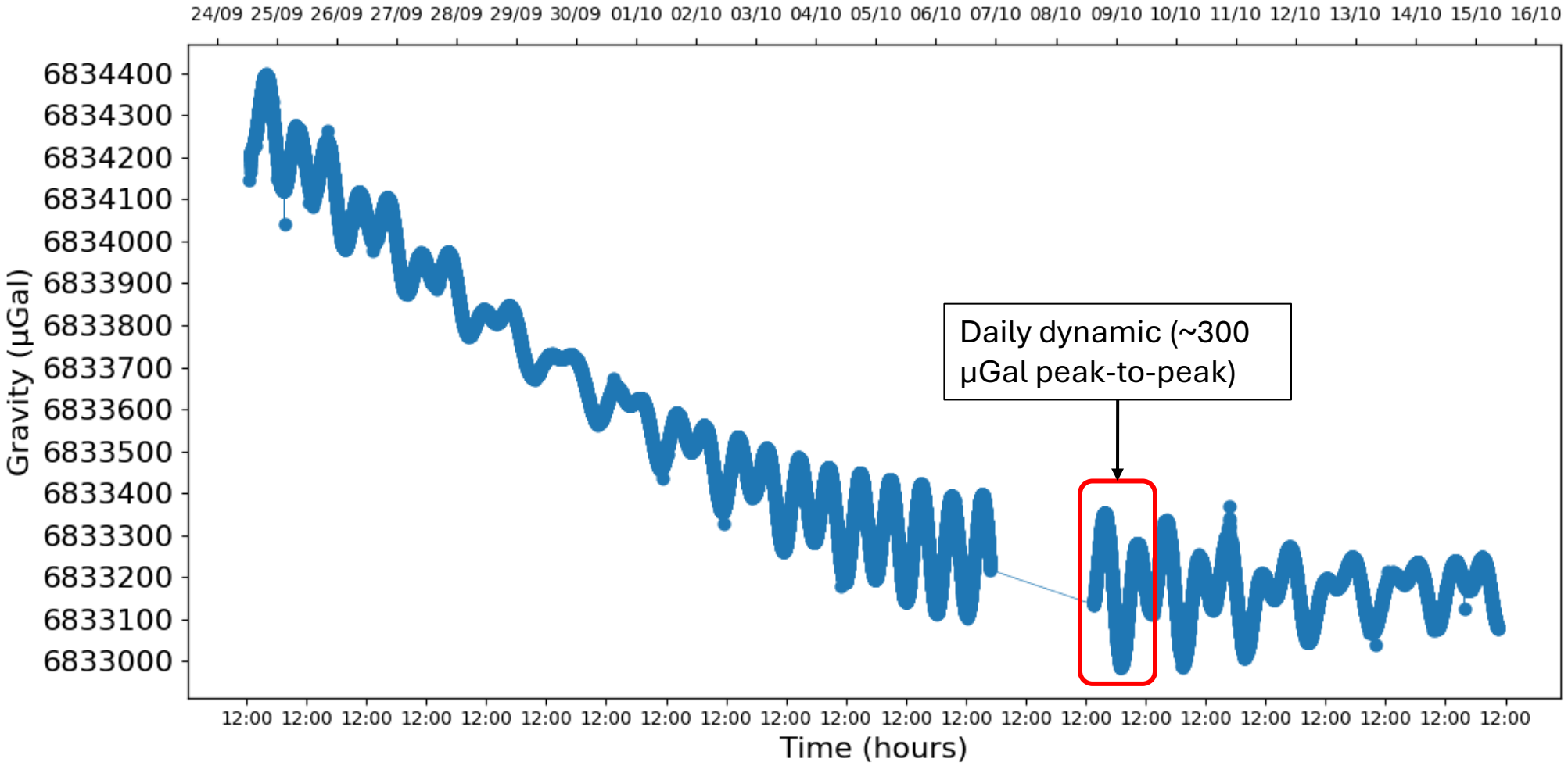

Dataset characteristics

- Duration: **21 days**
- Observations: **25500**
- Total variation: **1300 µGal**
- Standard deviation σ: **351 µGal**
- Mean daily dynamics: **~226 µGal**

Tide correction using the Longman model

The Longman formulation models solid Earth tides through the gravitational forcing of the Sun and Moon, expressed as a continuous function in time. It accurately captures short-period variability, allowing robust removal of diurnal and semidiurnal signals prior to drift analysis.

Source	Effective Period	Effect (µGal)	Longman Performance
Moon (dominant)	12–26 h (diurnal + semidiurnal envelope)	100–200	
Sun (dominant)	12–24 h	50–100	
Luni-solar interaction	~24 h modulation	30–80	
Ellipticity / declination effects	hours–days (continuous)	10–30	
Higher-order tidal components	hours–days	1–20	
Fortnightly modulation (Mf)	~14 days	1–5	
Monthly modulation (Mm)	~27 days	<1–3	

Longman model characteristics

- Physics-based model using Sun and Moon gravitational potential.
- Continuous formulation in time and space.
- Naturally reproduces diurnal and semidiurnal tides.
- Accurately removes dominant tidal signals (up to ~200 µGal).

Limitations in real data

- Higher-order components remain partially unresolved.
- Residual tidal signals: **~10–30 µGal.**
- Comparable to instrumental bias and environmental noise.

Effect of tidal correction on raw gravity data

Tidal correction effectively reduces short-period (diurnal) variability but has limited impact on the overall long-term trend.

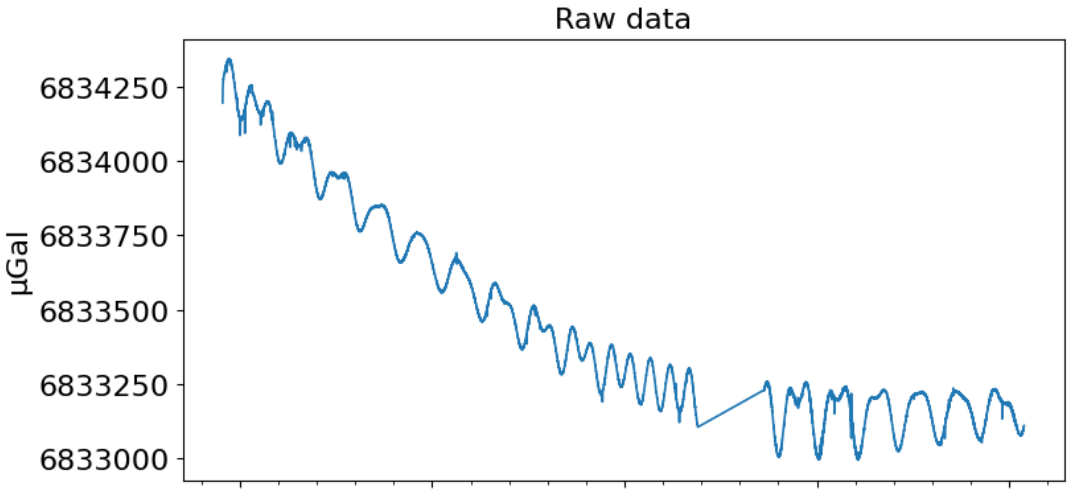

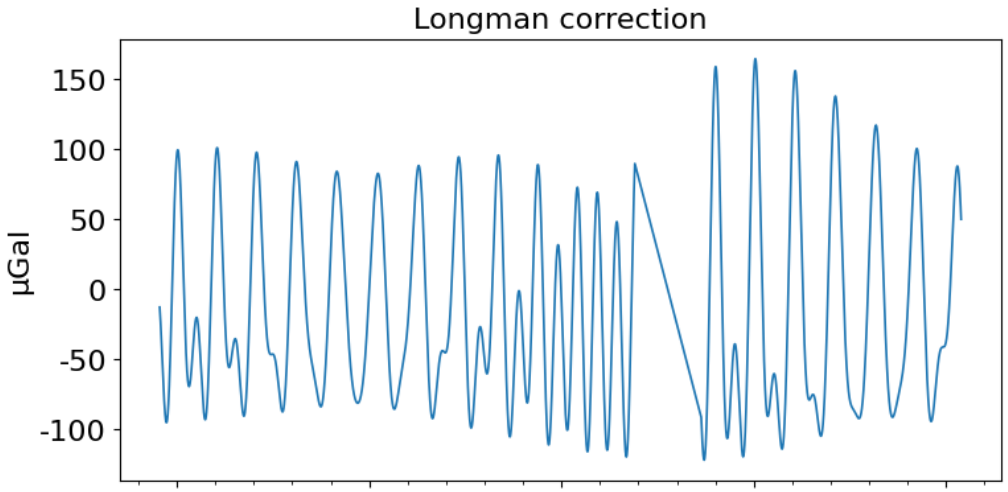

After tidal correction

- Standard deviation σ= **348 µGal**
- Mean daily dynamics= **84 µGal**

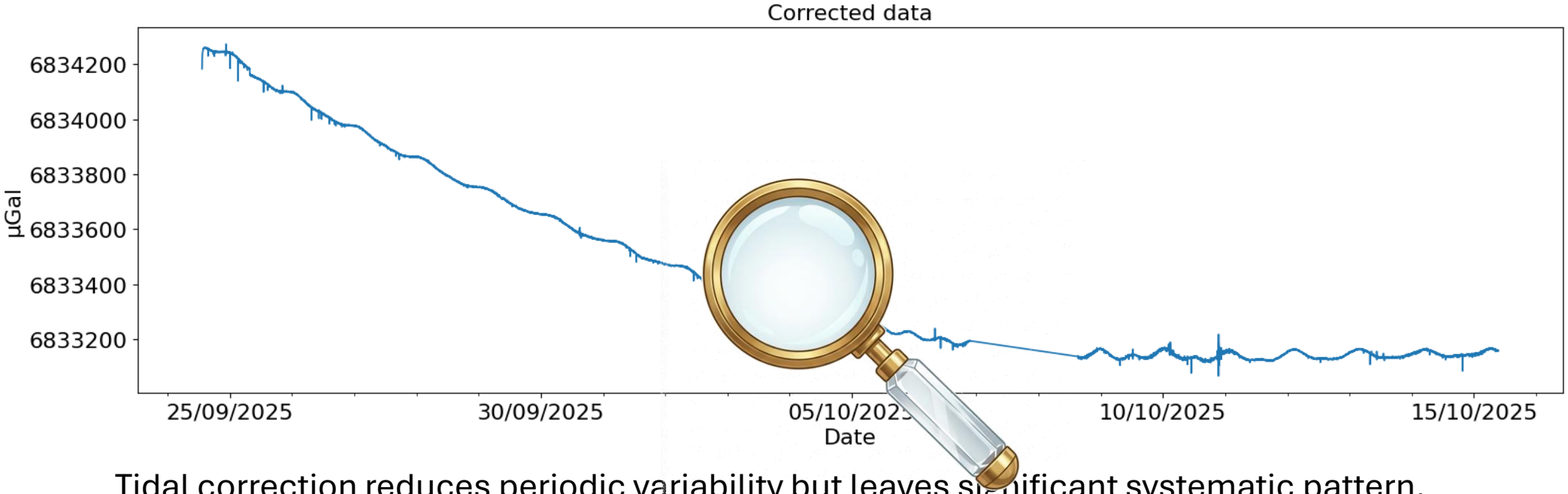

Tidal correction reduces periodic variability but leaves significant systematic pattern.

Iterative Harmonic Correction Framework (IHCF Model)

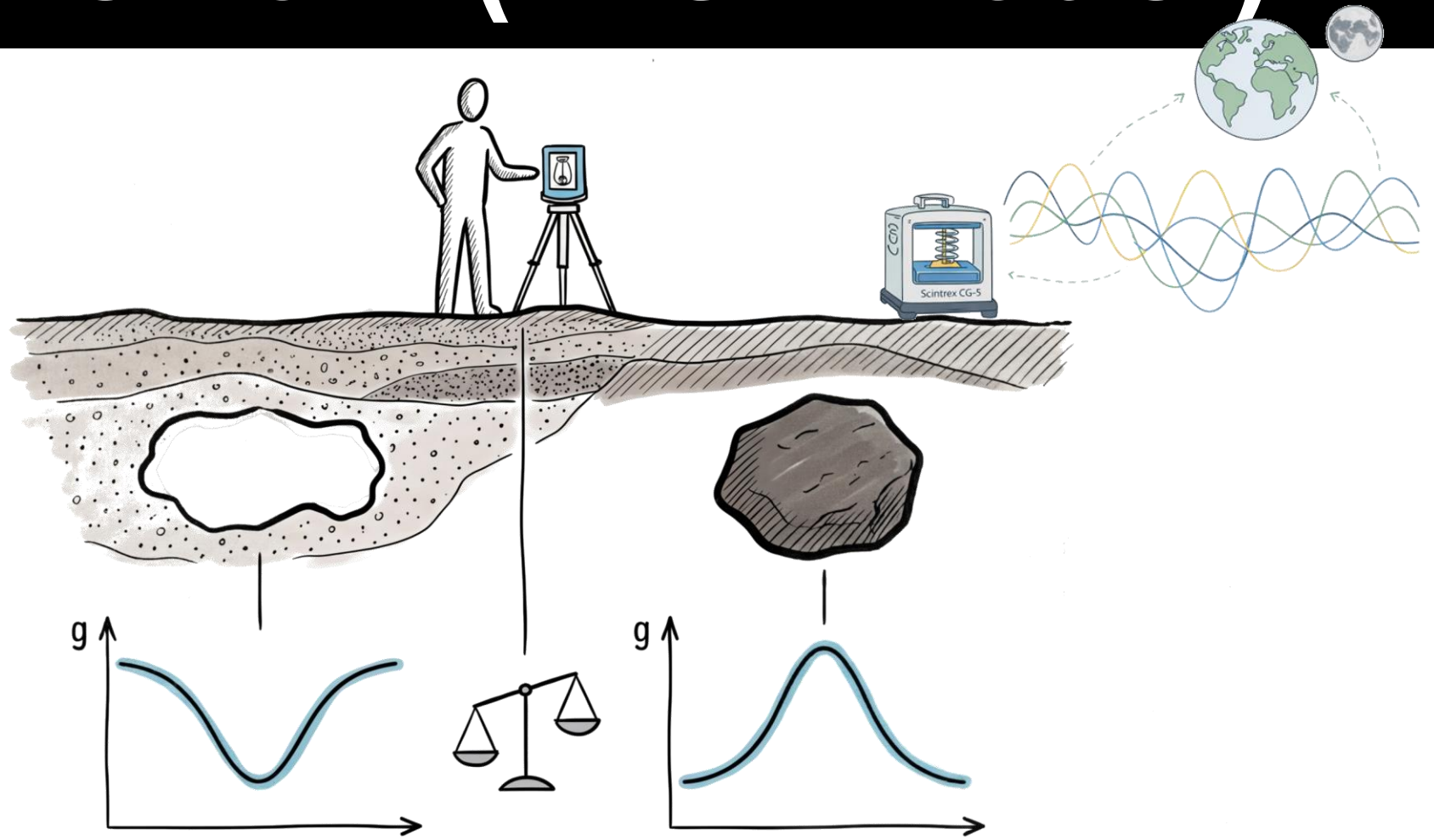

Iterative Harmonic Correction Framework (IHCF)

After memory and tidal corrections, the residuals still show time-correlated behavior. To capture these systematic patterns, an iterative harmonic model is applied, representing the signal as a sum of data-driven sinusoidal components.

$$g(t) = c + \sum_{j=1}^{k} [a_j \sin(\omega_j t) + b_j \cos(\omega_j t)]$$

k → Number of retained harmonic components

Definition of model parameters
• a_j, b_j : sine and cosine coefficients estimated by weighted least squares • $\omega_j = \frac{2\pi}{t_j}$: angular frequency • c: global offset

Frequency selection via competitive grid search
• Two period bands are explored: $T \in [0.5,4]$ days and $T \in [4,200]$ days. • Each band is discretized into candidate periods. • For each candidate period: coefficients are estimated via weighted least squares. • The best candidate in each band is selected based on minimum misfit. • A competition between bands selects the optimal component. • The component is accepted only if it significantly reduces the misfit. • The procedure is iteratively applied to residuals.

IHCF selection and model refinement

This flowchart represents the iterative scheme for searching periods in order to obtained the best fit according to statistical residuals.

Global stopping criterion: Iteration stops when residuals become statistically consistent with noise.

Component acceptance criterion: A harmonic component is retained only if the reduction in χ^2 exceeds a threshold that penalizes model complexity.

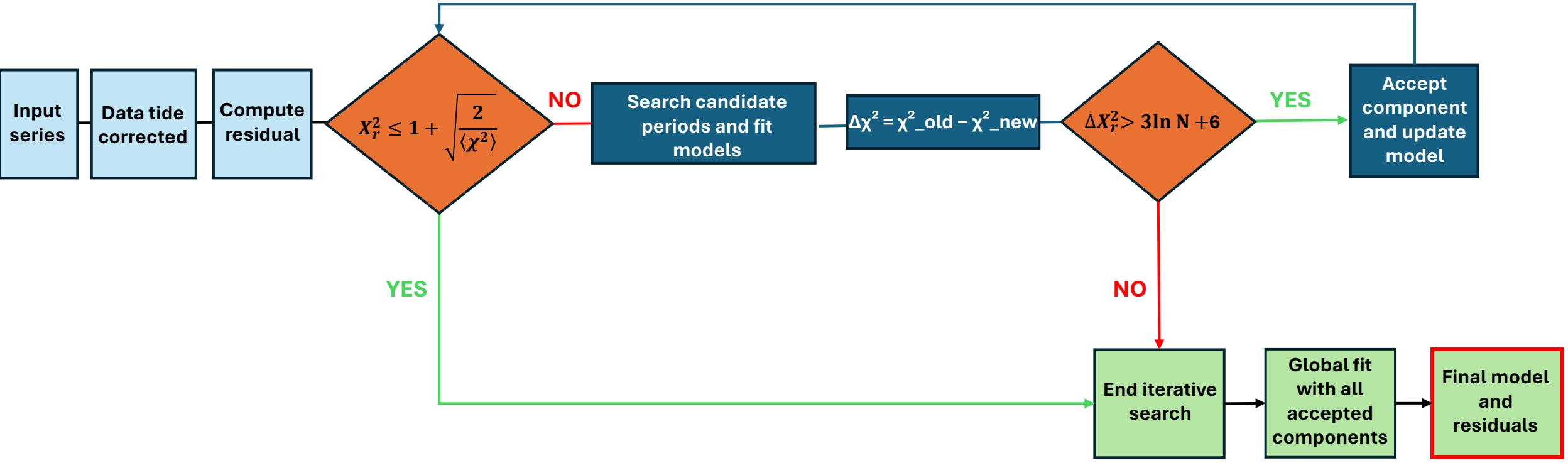

Validation of IHCF on San Giovanni dataset

Application of the proposed method to a continuous gravity dataset (San Giovanni test) to evaluate residual structure and

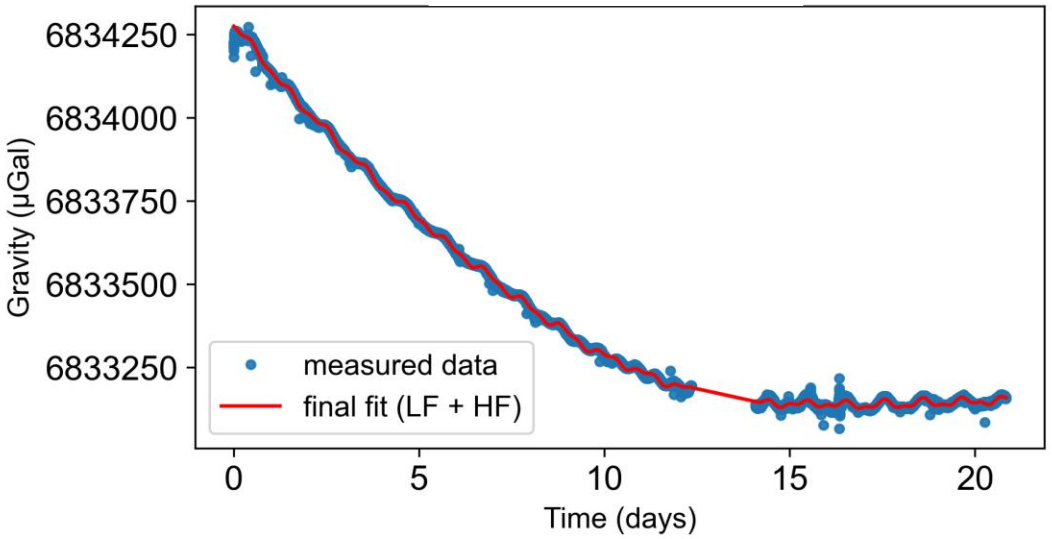

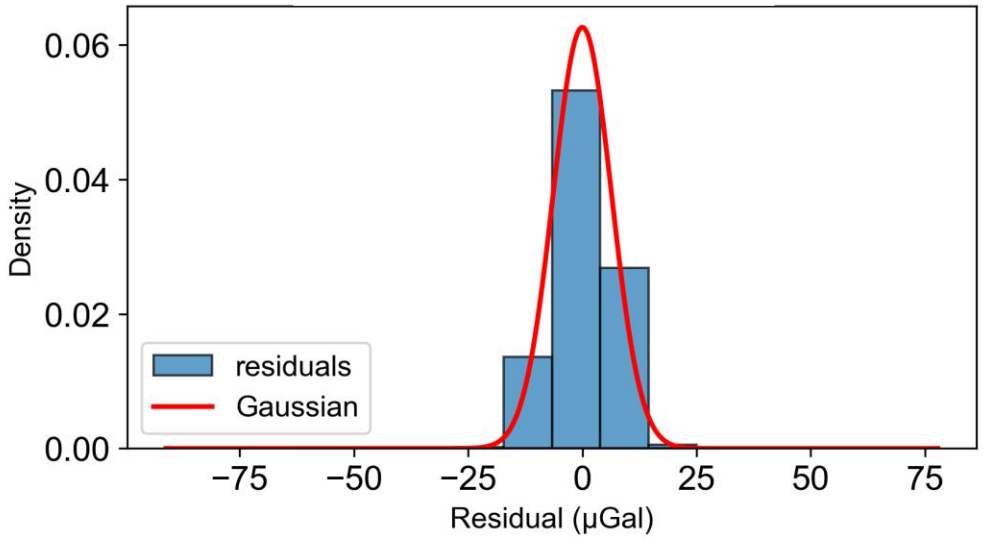

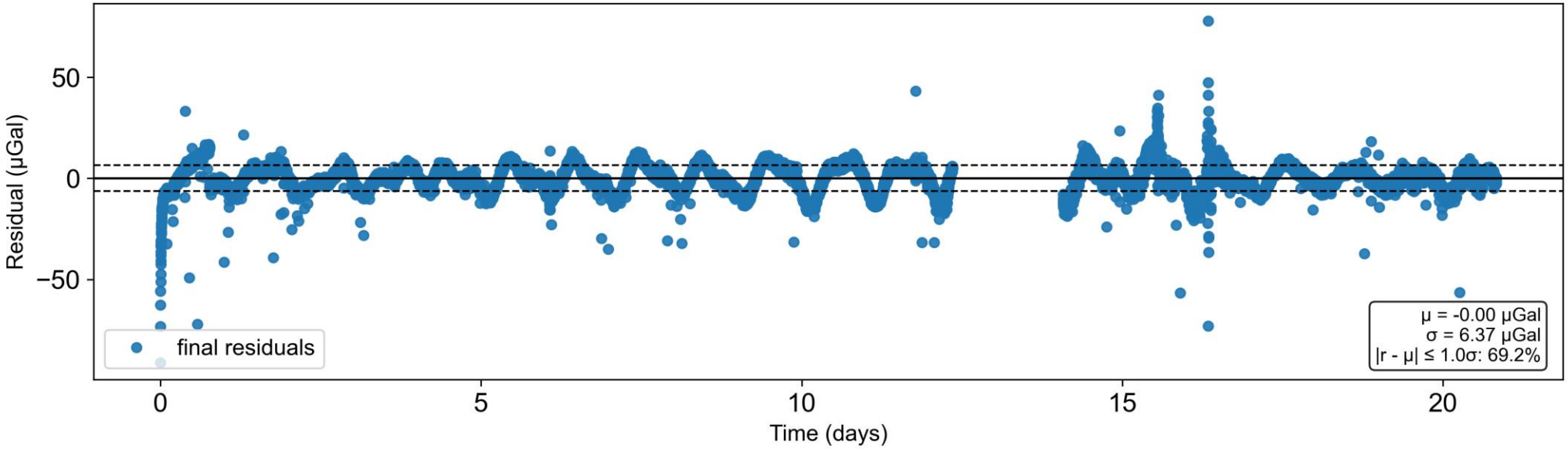

Key results

- μ ≈ 0 μGal.
- σ = 6.37 μGal.
- $X_r^2 \approx 1.1$
- Residuals follow a normal distribution.

Drift dominates the signal: why modeling is essential?

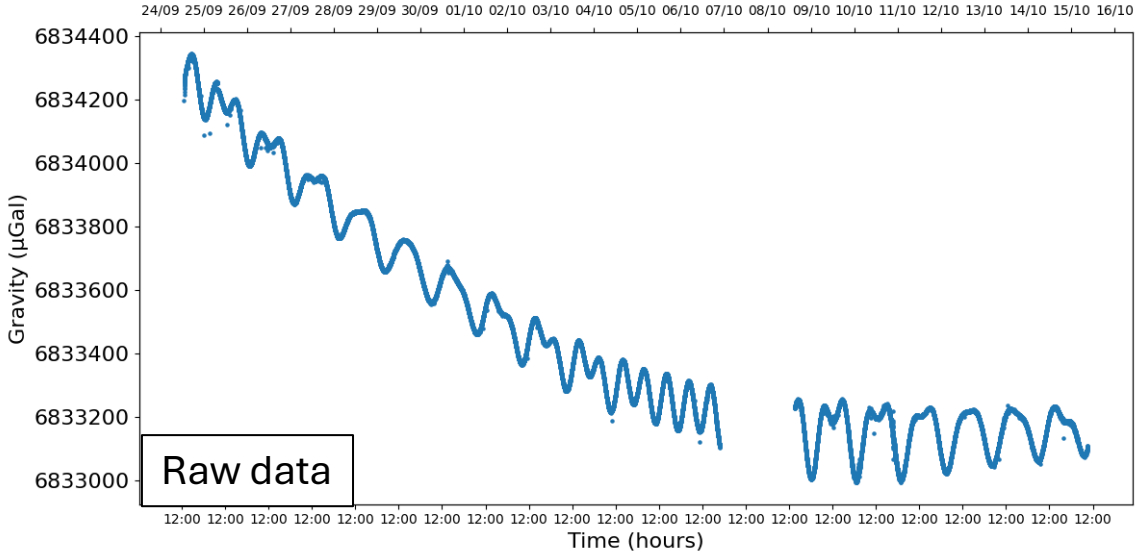

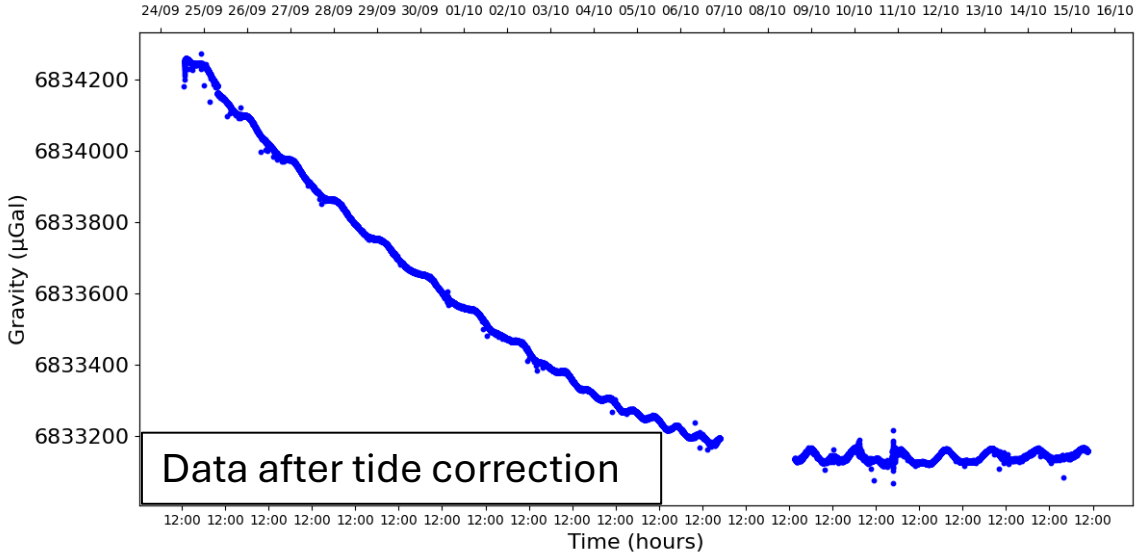

1. Daily reduction after tide removal: ~35%
2. Total reduction after IHCF: ~87%
3. Final reduced $\chi^2 \approx 1.1$

Most of the total variability is removed only after IHCF

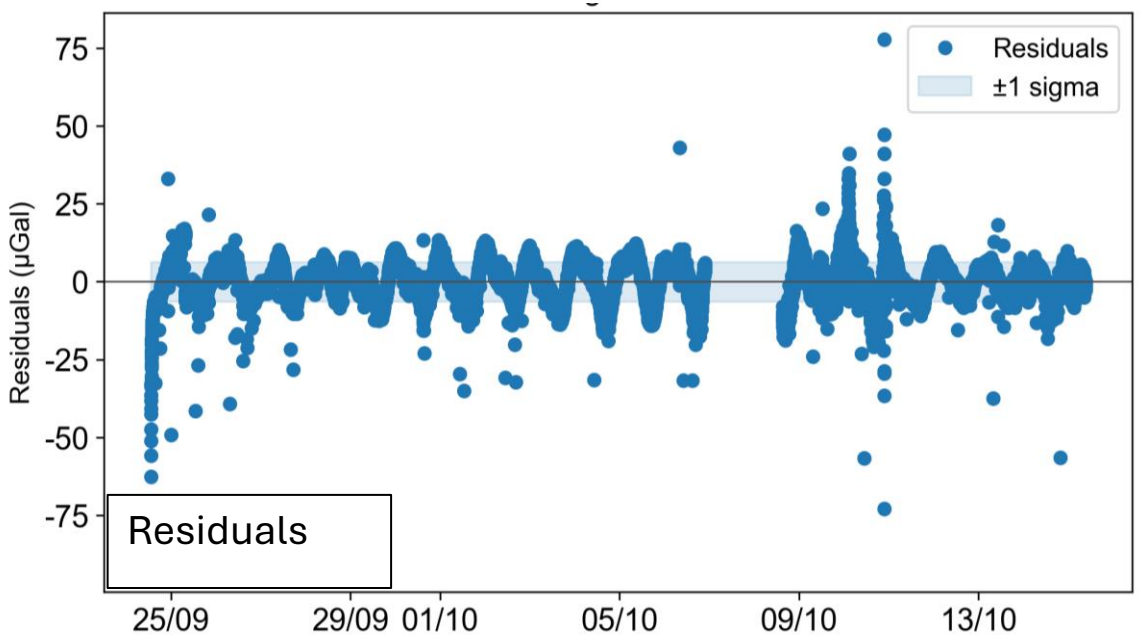

Residual variability after tide correction

Tide and memory-jump corrections reduce major artifacts, but significant variability and long-term trends remain in all datasets.

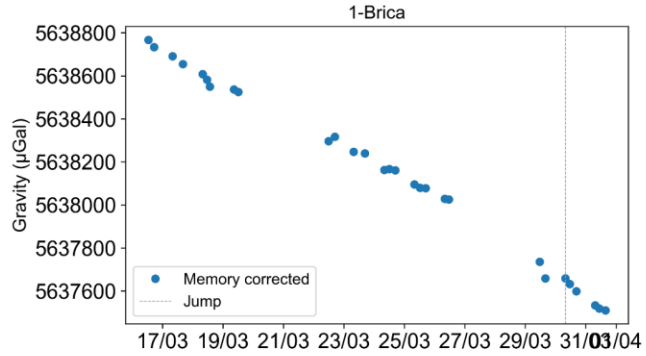

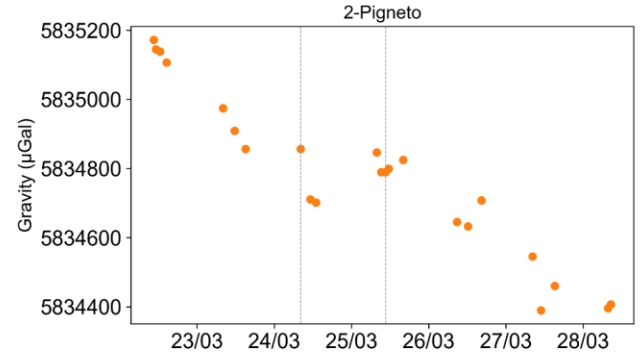

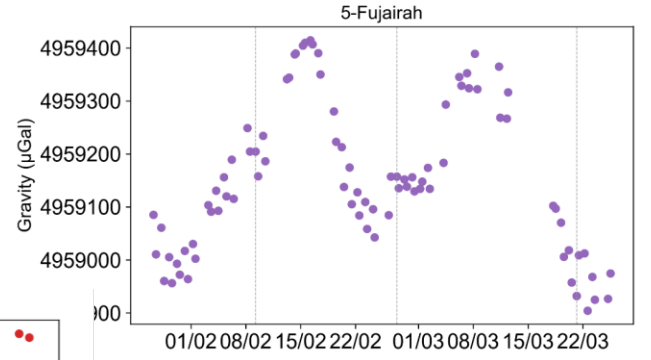

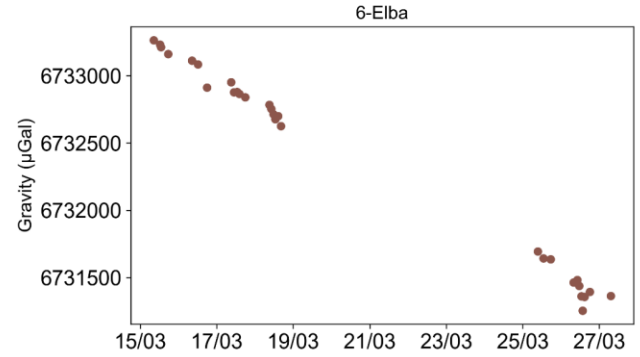

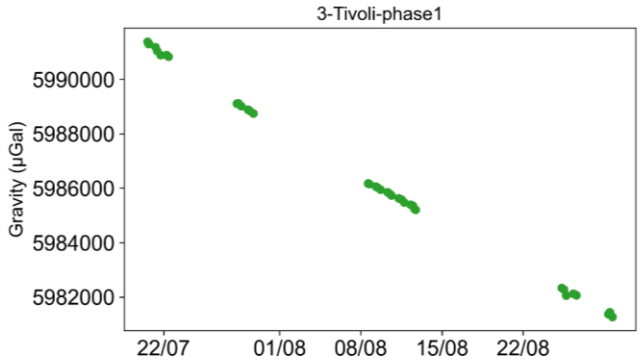

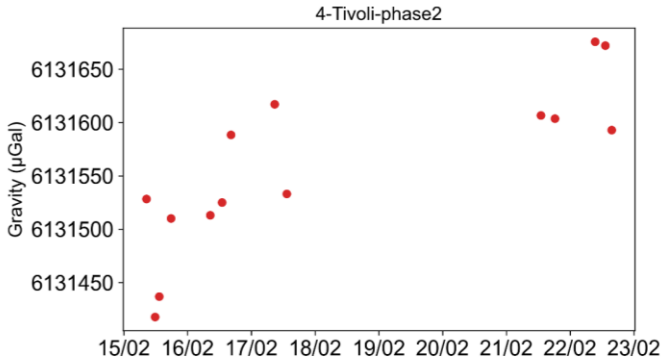

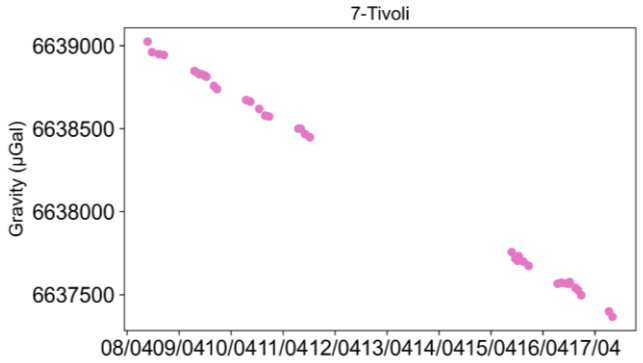

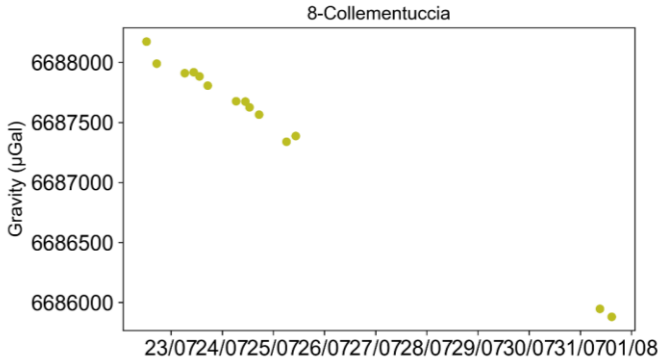

Key observations

- There are systematic patterns
- High residual variation over long period.
- Signal still dominated by systematic bias.

Final residual analysis after IHCF

Application of the full workflow to multiple field datasets to evaluate model performance and residual statistics across different environments.

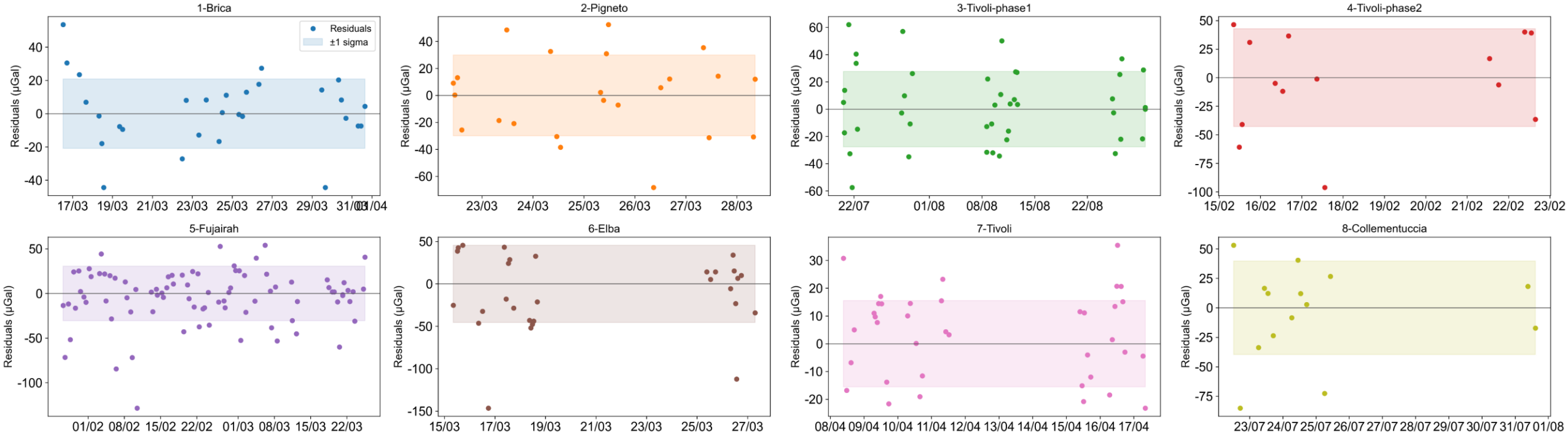

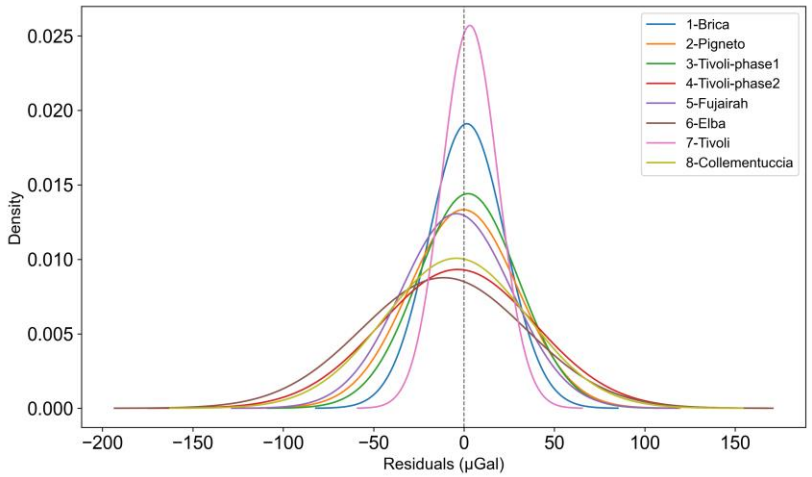

SITE ID	N. harmonic	RMSE (μGal)	X_v^2	μ (μGal)
1	1	20.6	1.8	1.6
2	3	29.2	0.7	-0.2
3	5	27.4	0.9	2.2
4	1	41.4	0.8	-3.5
5	11	30.6	3.2	-4.1
6	3	46.1	3.1	-11.2
7	1	15.6	0.4	3.2
8	1	38.4	0.7	-4.2

Residual noise vs anomaly amplitude: detection capability

Final residual noise levels are compared with typical microgravity anomaly amplitudes across application domains.

Final residual statistics	
Site ID	σ [µGal]
1	20.8
2	29.9
3	27.6
4	42.8
5	30.5
6	45.5
7	15.5
8	39.6
Average	31.6

Typical anomaly amplitudes	
Domain	Anomaly range (µGal)
Sinkhole	–30 to –50
Urban Subsurface Investigations	–50 to –100
Geotechnical Surveys	~30
Mineral Exploration	~1000
Volcanic Monitoring	–145 to +100
Environmental Monitoring	+10 to +50
Archaeological Prospection	+20 to +200
Geothermal Monitoring	+5 to +150

Key result:

- σ = 15–45 µGal.
- Comparable to anomaly amplitudes.
- Suitable for near-surface investigations.

The **ICHF workflow** reduces residual noise to levels suitable for all standard microgravity survey targets, ensuring applicability across diverse environments.

My results vs literature

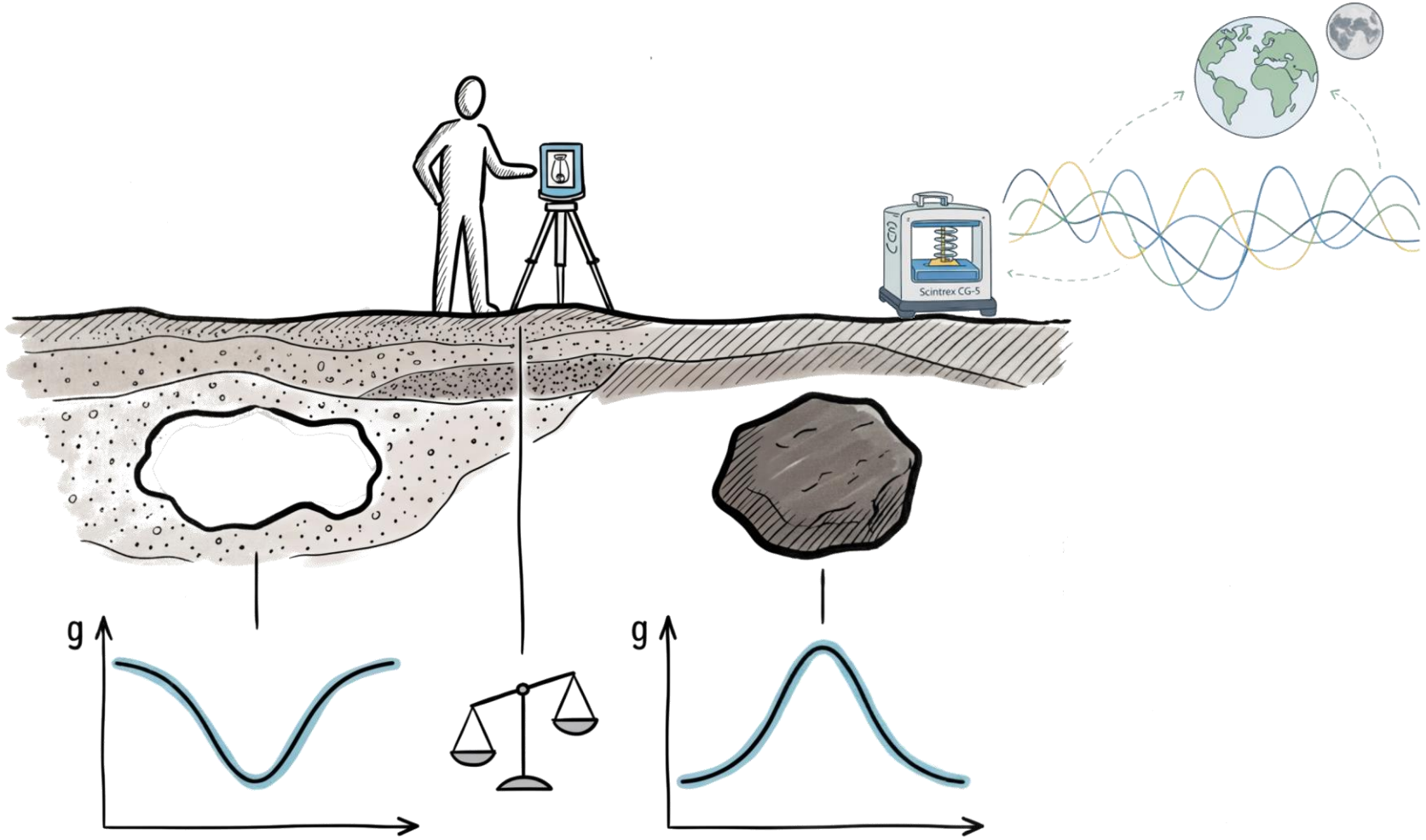

Microgravity strategies acquisition: Seigel vs IHCF approach

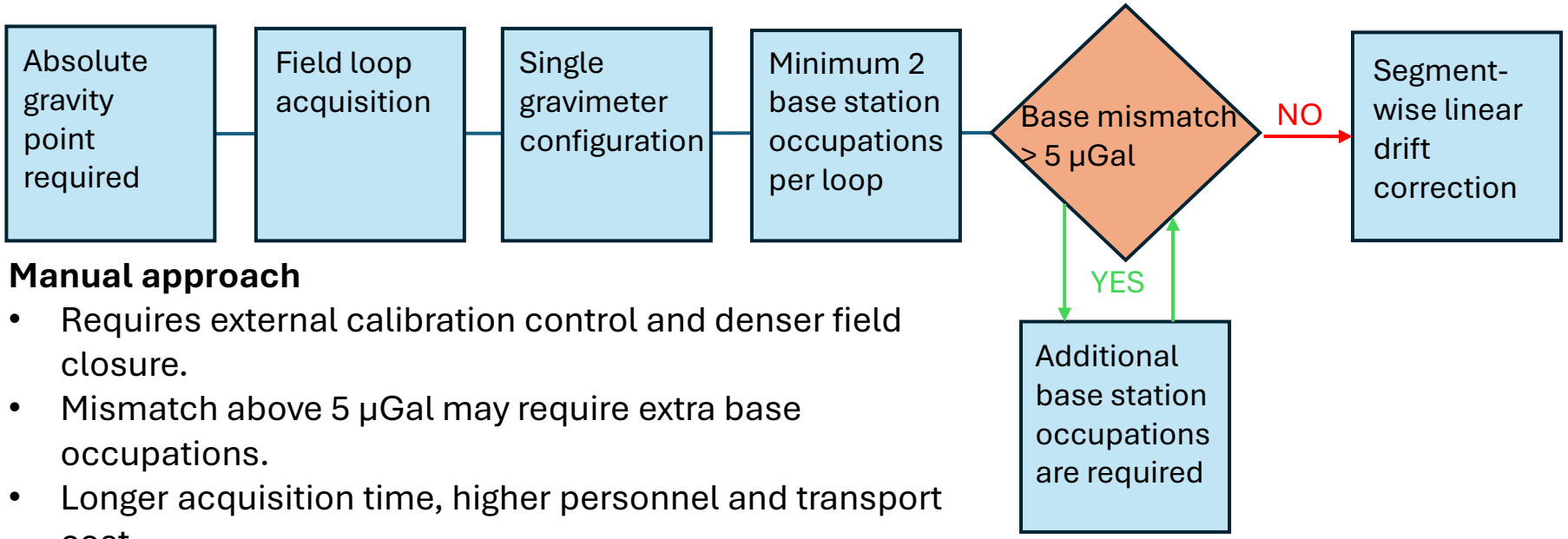

Manual approach

- Requires external calibration control and denser field closure.
- Mismatch above 5 µGal may require extra base occupations.
- Longer acquisition time, higher personnel and transport cost

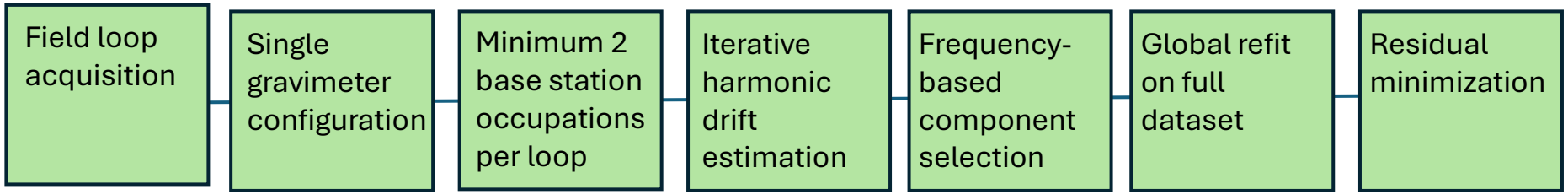

IHCF approach

- No external absolute reference required during acquisition.
- No additional loop extension driven by local base mismatch.
- Shorter acquisition time, lower operational cost.

Battaglia (2022) vs IHCF approach

The study by Battaglia et al. (2022) allow a direct quantitative comparison, as it reports field-based CG-5 performance under controlled acquisition and processing conditions, providing a reference benchmark for precision.

Context (Battaglia et al., 2022): Time-lapse microgravimetry for monitoring subsurface mass variations under controlled conditions

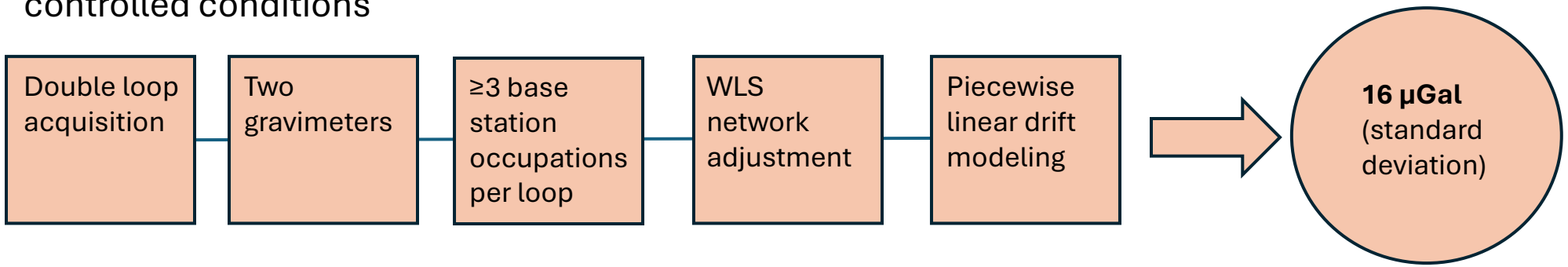

Context study thesis: Industrial microgravimetry for cavity detection in mining and complex environments, characterized by heterogeneous conditions and operational constraints.

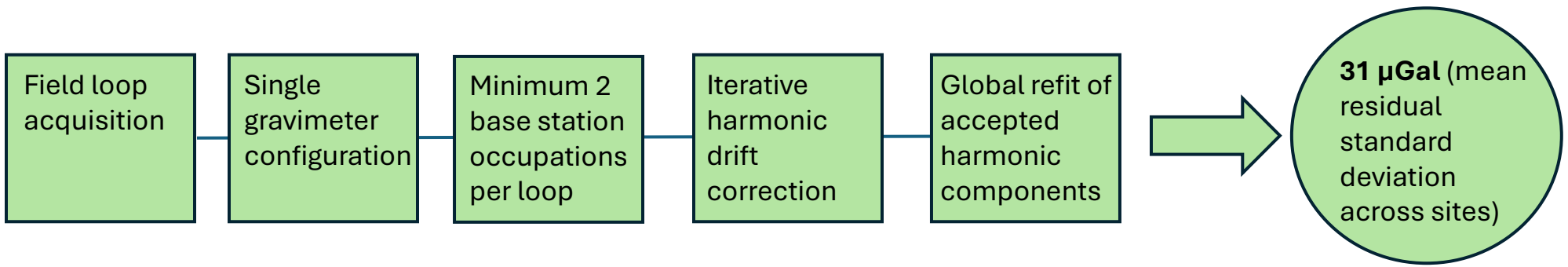

Comparable order of magnitude precision achieved under significantly less controlled conditions and reduced acquisition time.

Quadratic (Debeglia-type) vs IHCF approach

Debeglia and Dupont (2002) indicate that long-term instrumental drift in relative gravimeters may include higher-order components, which can be approximated using low-order polynomial models. Here, a second-order polynomial drift correction is compared with a harmonic model using the San Giovanni continuous dataset.

QUADRATIC FIT (Debeglia): $g(t) = a + bt + ct^2$

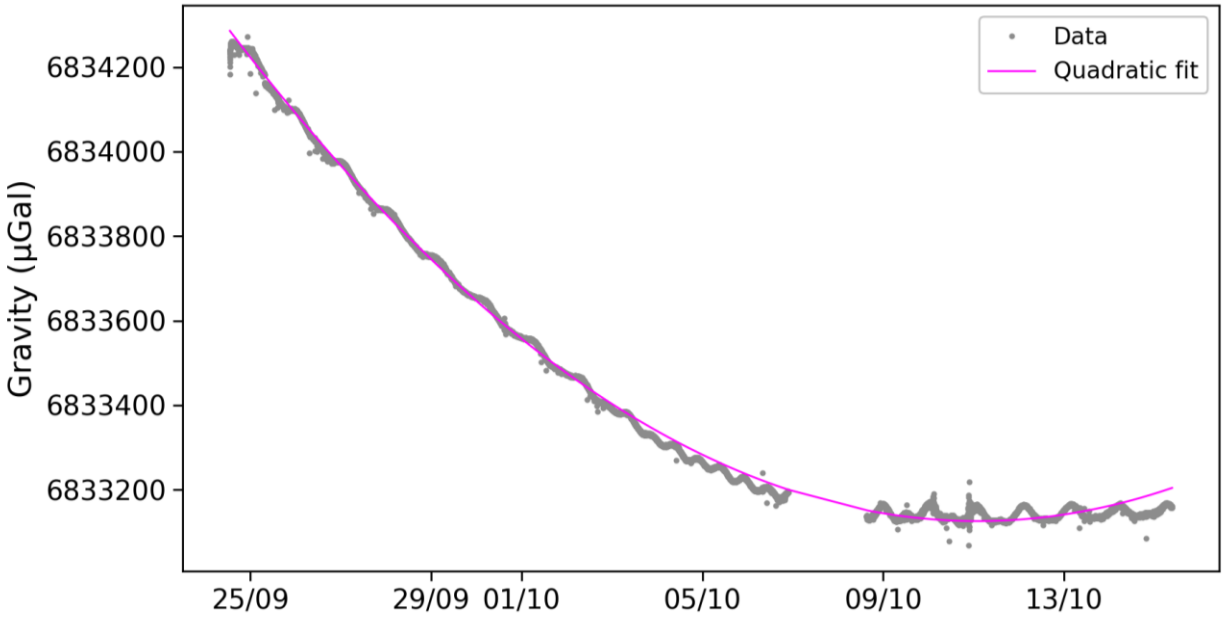

Standard deviation of residual = 16.11 µGal

HARMONIC FIT: $g(t) = c + \sum_{j=1}^{k}[a_j \sin(\omega_j t) + b_j \cos(\omega_j t)]$

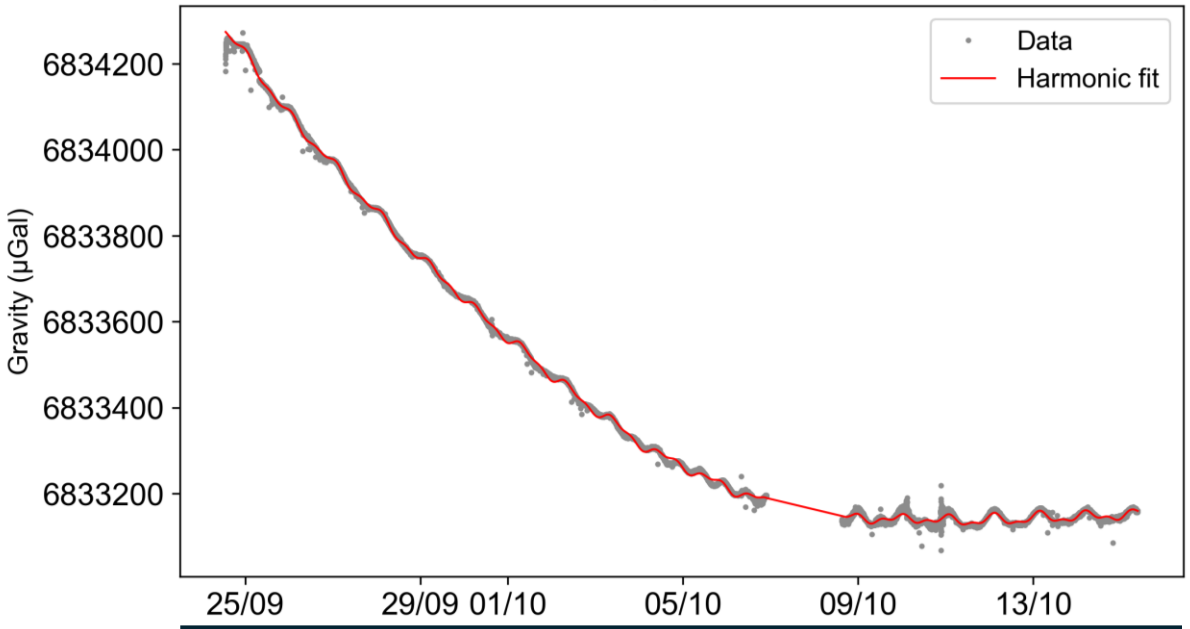

Standard deviation of residual = 6.37 µGal

The quadratic model fails to capture short-term variability in CG-5 drift, while a harmonic component significantly improves the fit, suggesting the presence of quasi-periodic instrumental or environmental contributions not accounted for by polynomial models

High-order polynomial (Elsaka-type) vs IHCF approach

Elsaka (2020) models instrumental drift using high-order polynomials, showing that a 6th-degree fit minimizes residual variance in controlled CG-5 datasets. Here we compare this approach with a harmonic model applied to continuous data.

POLYNOMIAL FIT (Elsaka): $g(t) = a_0 + a_1 t + a_2 t^2 + \cdots + a_6 t^6$

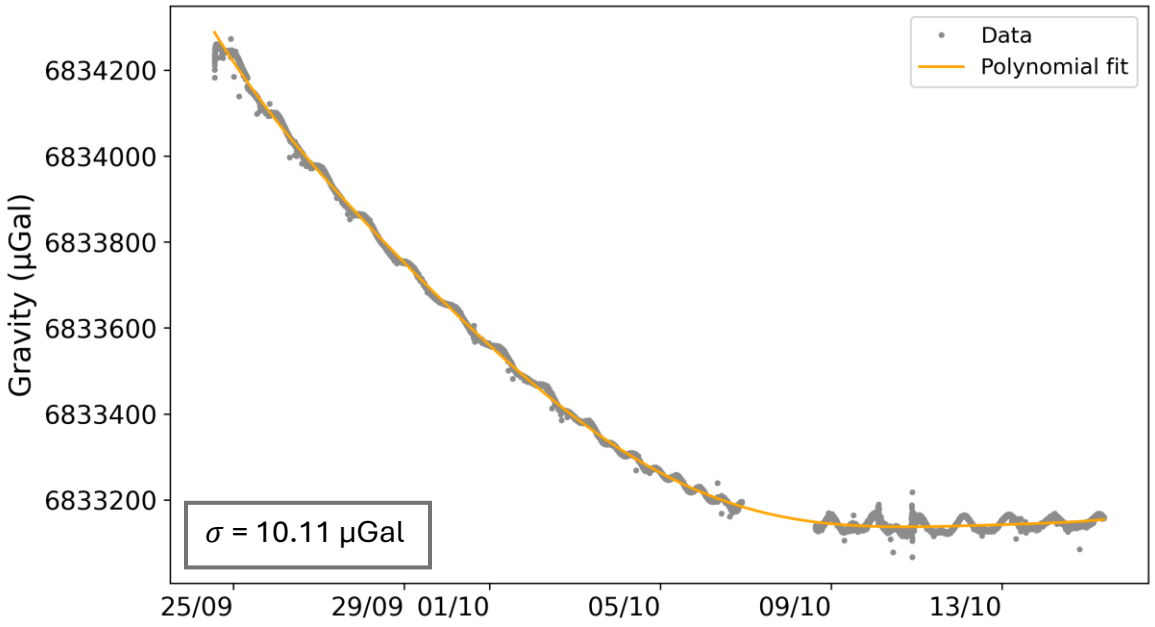

HARMONIC FIT: $g(t) = c + \sum_{j=1}^{k} [a_j \sin(\omega_j t) + b_j \cos(\omega_j t)]$

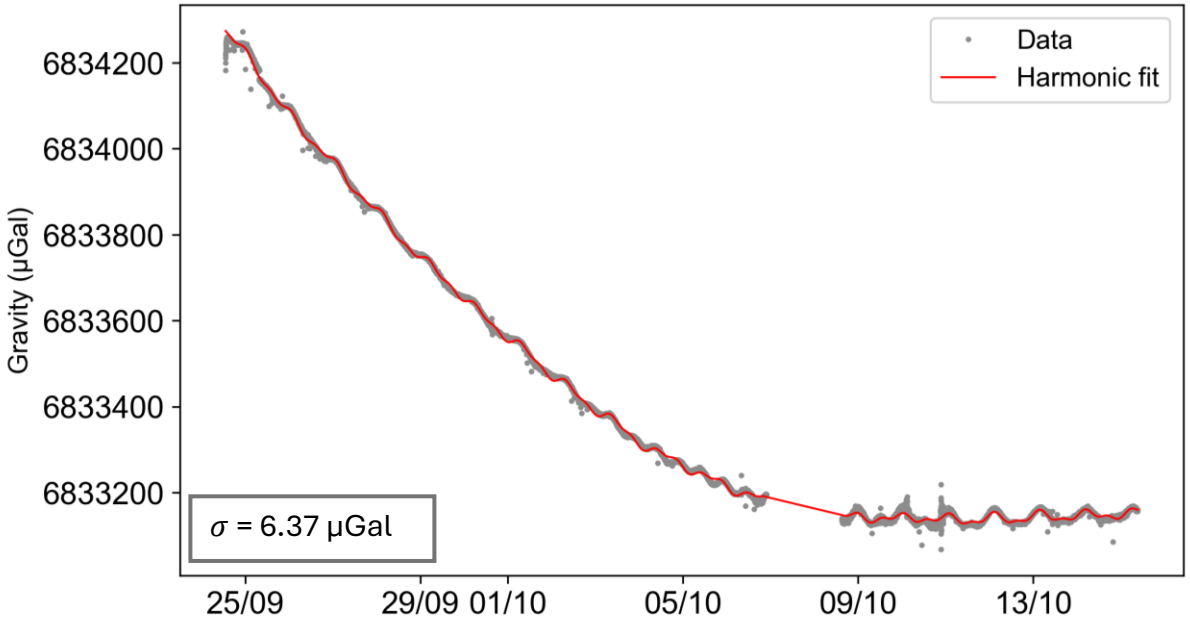

Limitations of polynomial approach

- Validated mainly in laboratory conditions.
- Degree selection driven by variance minimization.
- Tends to favor high-order models.
- Not reliable for sparse campaigns.

Polynomial models improve drift estimation but fail to capture short-term variability. The harmonic approach provides a better fit, suggesting quasi-periodic instrumental or environmental contributions.

Conclusions and impacts

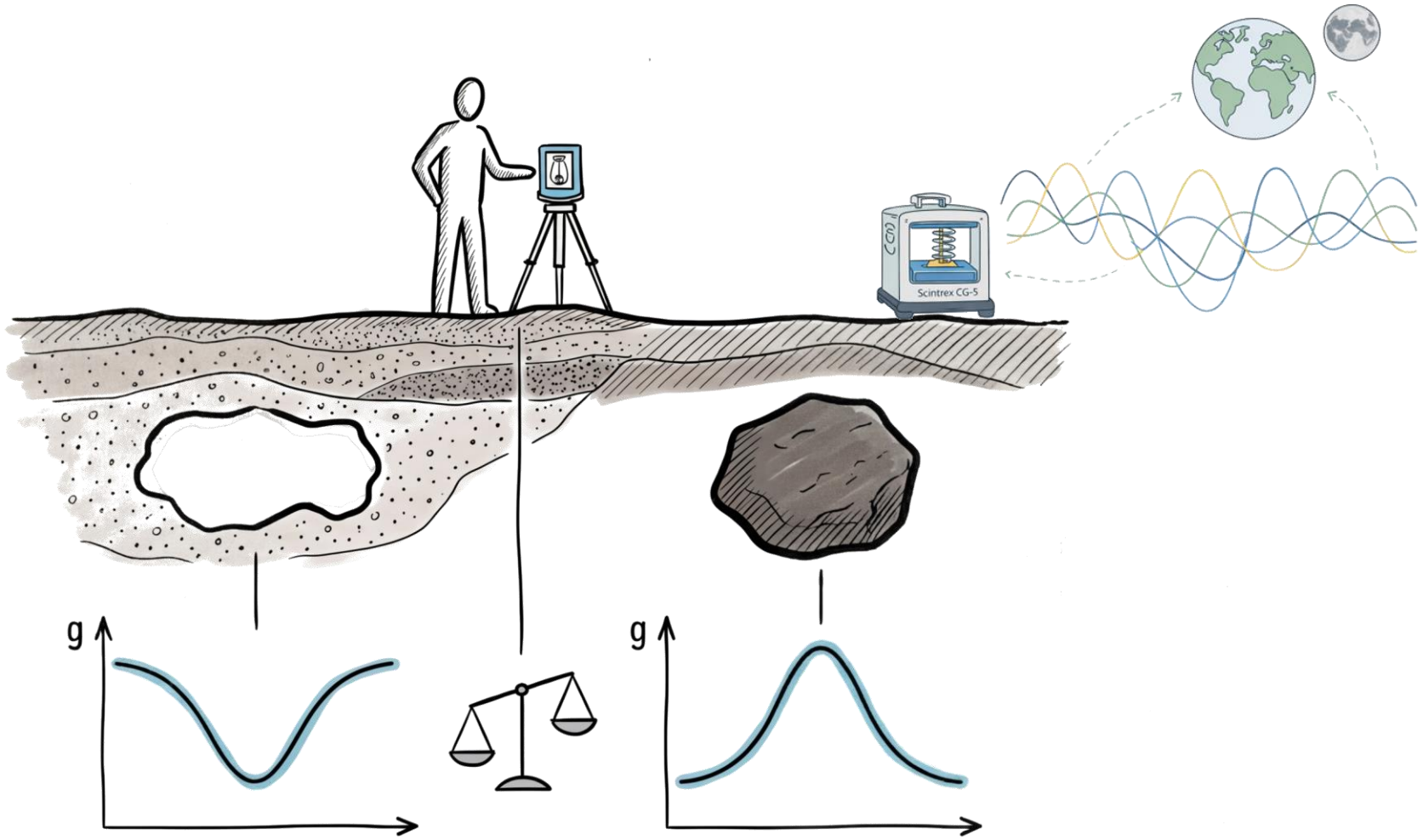

Challenges addressed and solutions developed in this research

Instrumental discontinuity correction
Memory offsets and instrumental resets were identified and corrected, removing discontinuities (~250 µGal) and ensuring a robust basis for subsequent drift modelling.

Limits of tidal correction
It was demonstrated that, in multi day acquisitions, the Longman model does not remove all systematic components, leaving a residual daily variability (~100 µGal).

Advanced harmonic modelling
Residuals consistently exhibited harmonic structures, captured through multi sinusoidal decomposition, reducing uncertainty below ~ 30 µGal and ensuring instrumental repeatability.

Noise floor achievement
The developed **algorithm removed systematic components** down to the noise floor, providing optimal data for the geological interpretation pipeline.

Component / Process	Residual amplitude
Raw signal variability	~1000 µGal
After memory correction	~250 µGal
After tide correction	~100 µGal
After harmonic model	~30 µGal

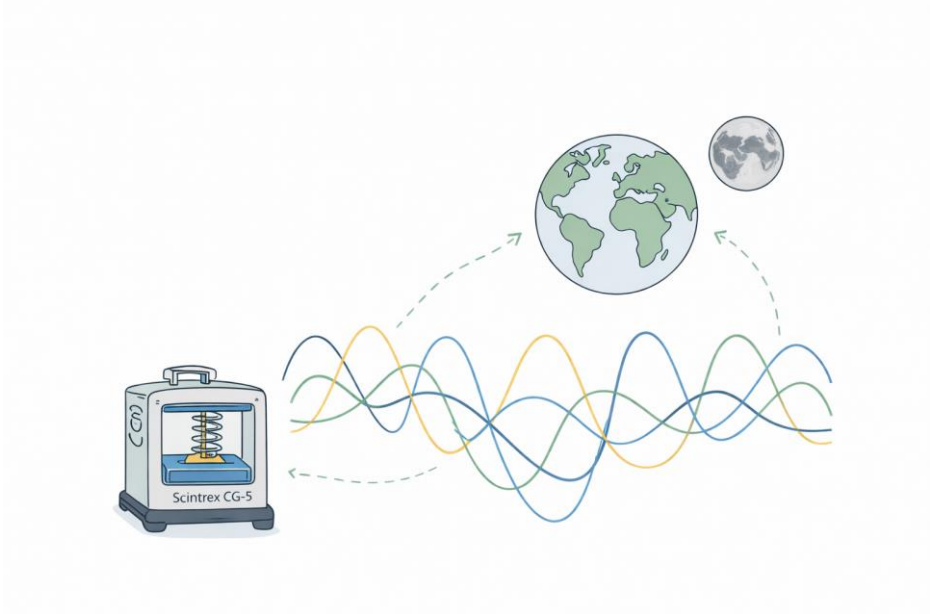

A paradigm shift in GeoExplorer data processing

Old legacy workflow (Pre PhD)

- Expert dependent manual drift correction workflow execution.
- Operator driven subjective correction decision making.
- Limited reproducibility across operators, surveys, and datasets.
- No explicit uncertainty modeling or error propagation framework.
- Post processing cost 25% of survey, requiring expert operators.

New GeoExplorer workflow (Post PhD)

- Assignable to non expert operators, standardized workflow execution.
- Quantitative, model driven, objective correction decision process.
- Fully reproducible and scalable across surveys and datasets.
- Explicit uncertainty estimation and residual error quantification.
- Post processing is reduced to 4% of the total microgravimetry survey.

GEOExplorer

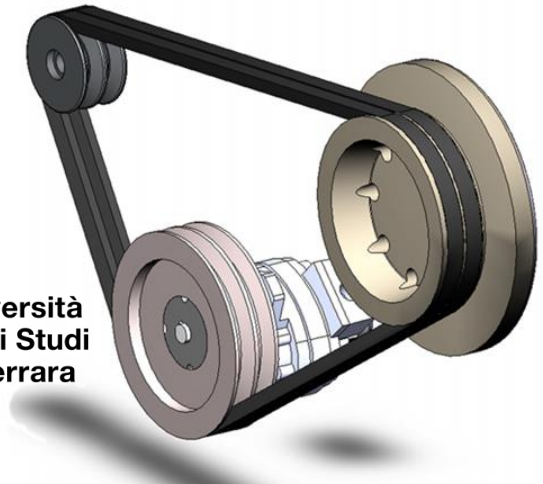

Università degli Studi di Ferrara

Through my PNRR PhD, real technology transfer to GeoExplorer has been achieved.

Thank you for your attention